1521-0111/12/8205-843–859$25.00
MOLECULAR PHARMACOLOGY
Vol. 82, No. 5
79640/3799625

Mol Pharmacol 82:843–859, 2012

Identification and Pharmacological Characterization of Multiple Allosteric Binding Sites on the Free Fatty Acid 1 Receptor[S]

Daniel C.-H. Lin, Qi Guo, Jian Luo, Jane Zhang, Kathy Nguyen, Michael Chen, Thanh Tran, Paul J. Dransfield, Sean P. Brown, Jonathan Houze, Marc Vimolratana, Xian Yun Jiao, Yingcai Wang, Nigel J. M. Birdsall, and Gayathri Swaminath

Amgen Inc., South San Francisco, California (D.C.-H.L., Q.G., J.L., J.Z., K.N., M.C., T.T., P.J.D., S.P.B., J.H., M.V., X.Y.J., Y.W., G.S.); and Division of Physical Biochemistry, MRC National Institute for Medical Research, London, United Kingdom (N.J.M.B.)

Received April 26, 2012; accepted August 2, 2012

ABSTRACT

Activation of FFA1 (GPR40), a member of G protein-coupling receptor family A, is mediated by medium- and long-chain fatty acids and leads to amplification of glucose-stimulated insulin secretion, suggesting a potential role for free fatty acid 1 (FFA1) as a target for type 2 diabetes. It was assumed previously that there is a single binding site for fatty acids and synthetic FFA1 agonists. However, using members of two chemical series of partial and full agonists that have been identified, radioligand binding interaction studies revealed that the full agonists do not bind to the same site as the partial agonists but exhibit positive heterotropic cooperativity. Analysis of functional data reveals positive functional cooperativity between the full agonists and partial agonists in various functional assays (in vitro and ex vivo) and also in vivo. Furthermore, the endogenous fatty acid docosahexaenoic acid (DHA) shows negative or neutral cooperativity with members of both series of agonists in binding assays but displays positive cooperativity in functional assays. Another synthetic agonist is allosteric with members of both agonist series, but apparently competitive with DHA. Therefore, there appear to be three allosterically linked binding sites on FFA1 with agonists specific for each of these sites. Activation of free fatty acid 1 receptor (FFAR1) by each of these agonists is differentially affected by mutations of two arginine residues, previously found to be important for FFAR1 binding and activation. These ligands with their high potencies and strong positive functional cooperativity with endogenous fatty acids, demonstrated in vitro and in vivo, have the potential to deliver therapeutic benefits.

Introduction

The FFA1 receptor (GPR40) is closely related to the other fatty acid receptors, FFA2 and FFA3 (Sawzdargo et al., 1997; Stoddart et al., 2008). The members of this family share an overall sequence homology of 30 to 50% and higher within their putative transmembrane domains (Costanzi et al., 2008; Swaminath, 2008). Free fatty acids are not only an integral component of cells, but they also function as signaling molecules. Several reports have demonstrated that the FFA1 receptor is activated by both medium- and long-chain fatty acids (Briscoe et al., 2003; Itoh et al., 2003) and couples preferentially to $G\alpha_q$ (Latour et al., 2007; Stoddart et al., 2007) to stimulate phospholipase C activity (Briscoe et al., 2003).

It has been demonstrated that FFA1 receptors are expressed in brain and monocytes and, importantly, in the pancreas, especially in β-cells. Studies suggest that FFA1 plays a significant role in the chain of events linking obesity

The work was supported in part by the Medical Research Council, United Kingdom [Grant U117532193].

D.C.-H.L., Q.G., J.L., and G.S. contributed equally to the work.

This work was previously presented in part in the following publication: Guo Q, Zhang J, Dransfield PJ, Brown SP, Houze JH, Vimolratana M, Jiao XY, Sun Y, Wang Y, Birdsall NJM, et al. Identification and pharmacological characterization of multiple allosteric binding sites on the FFA1R. *Keystone Symposium on G Protein-Coupled Receptors*, 2010 7–12 April; Breckenridge, CO.

N.J.M.B. has been a paid consultant for AMGEN Inc.

Article, publication date, and citation information can be found at http://molpharm.aspetjournals.org.

http://dx.doi.org/10.1124/mol.112.079640.

[S] The online version of this article (available at http://molpharm.aspetjournals.org) contains supplemental material.

ABBREVIATIONS: FFA, free fatty acid; GPC, G protein-coupled fatty acid receptor; TAK-875, [(3*S*)-6-({2′,6′-dimethyl-4′-[3-(methylsulfonyl)propoxy]biphenyl-3-yl}methoxy)-2,3-dihydro-1-benzofuran-3-yl]acetic acid hemi-hydrate; AMG 837, (*S*)-3(-4-((4′-(trifluoromethyl)-[1,1′-biphenyl]-3-yl)methoxy) phenyl)hex-4-ynoic acid; DHA, docosahexaenoic acid; FFAR1, free fatty acid receptor 1; AM 1638, (*S*)-3-cyclopropyl-3-(3-((2-(5,5-dimethylcyclopent-1-en-1-yl)-2′-fluoro-5′-methoxy-[1,1′-biphenyl]-4-ylmethoxy) phenyl)propanoic acid; AM 8182, (*S*,*E*)-3-(4-((2′-fluoro-5′-methoxy-[1,1′-biphenyl]-4-yl)methoxy) phenyl)hex-4-enoic acid); AM 6331 (*S*)-3-(4-((4′-chloro-2′-ethoxy-[1,1′-biphenyl]-4-yl)methoxy phenyl)hex-4-ynoic acid; HBSS, Hanks' buffered salt solution; ERK, extracellular signal-regulated kinase; BSA, bovine serum albumin; HSA, human serum albumin; CHO, Chinese hamster ovary; hFFA, human FFA; FACS, fluorescence-activated cell sorting; STZ, streptozotocin; IP, inositol phosphate; SAR, structure-activity relationship; GPCR, G protein-coupled receptor; LA, α-linolenic acid; HF/STZ, high-fat STZ-treated; ANOVA, analysis of variance; GW9508, 4-[[(3-phenoxyphenyl)methyl]amino]benzenepropanoic acid.

and type 2 diabetes (Steneberg et al., 2005), although recent reports dispute this claim (Kebede et al., 2008; Lan et al., 2008; Alquier et al., 2009). Activation of the FFA1 receptor by fatty acids stimulates insulin secretion in a glucose-dependent manner in the Min6 cell line (Itoh and Hinuma, 2005), and transgenic expression of GPR40 in pancreatic β-cells results in improved glucose tolerance and enhanced insulin secretion induced by a high-fat diet (Nagasumi et al., 2009).

A number of potent GPR40 synthetic ligands have been reported (Christiansen et al., 2008; Sasaki et al., 2011; Walsh et al., 2011), including two agonists that have entered the clinic, [(3*S*)-6-({2′,6′-dimethyl-4′-[3-(methylsulfonyl)propoxy]biphenyl-3-yl}methoxy)-2,3-dihydro-1-benzofuran-3-yl]acetic acid hemi-hydrate (TAK-875) (Araki et al., 2012; Naik et al., 2012) and (*S*)-3(-4-((4′-(trifluoromethyl)-[1,1′-biphenyl]-3-yl)methoxy) phenyl) hex-4-ynoic acid (AMG 837) (Lin et al., 2011).

In this study, we report members of two series of novel synthetic agonists that display full or partial agonism at the FFA1 receptor relative to that of an endogenous ligand, DHA. Two radioligands have been synthesized, and this has allowed the complex allosteric interactions between the synthetic agonists and with DHA to be quantitated. Three distinct allosterically linked binding sites for FFAR1 agonists are postulated. To our knowledge, this is the first measurement of the binding properties of FFAR1 ligands using a radioligand binding assay. The interactions have been explored further in various in vitro and in vivo functional assays.

Two arginine residues, Arg183(5.39) and Arg258(7.35), have been considered to be key residues in both receptor activation and in the binding of the carboxyl group present in most FFAR1 agonists (Sum et al., 2007, 2009; Tikhonova et al., 2007; Smith et al., 2009). The differential effects of the mutation of these residues on the activation of FFAR1 by ligands that bind to each of the binding sites have been explored.

These studies not only provide an insight into the underlying mechanisms of binding and activation of FFA1 receptor but also highlight the potential importance of allosteric FFA1 agonists as therapeutic agents to treat type 2 diabetes.

Materials and Methods

Materials. AMG 837, (*S*)-3-cyclopropyl-3-(3-((2-(5,5-dimethylcyclopent-1-en-1-yl)-2′-fluoro-5′-methoxy-[1,1′-biphenyl]-4-ylmethoxy) phenyl)propanoic acid (AM 1638), (*S*,*E*)-3-(4-((2′-fluoro-5′-methoxy-[1,1′-biphenyl]-4-yl)methoxy)phenyl)hex-4-enoic acid) (AM 8182), and (*S*)-3-(4-((4′-chloro-2′-ethoxy-[1,1′-biphenyl]-4-yl)methoxy phenyl)hex-4-ynoic acid (AM 6331) were synthesized at Amgen Inc. (South San Francisco, CA). Details of their syntheses and characterization are described elsewhere (Brown et al., 2011; Lin et al., 2011; Walker et al., 2011). All other reagents were purchased from the following vendors. [^{3}H]AMG 837 (80Ci/mmol) was synthesized by American Radiolabeled Chemicals Inc. (St. Louis, MO). [^{3}H]AM 1638 (31.4Ci/mmol) was synthesized by Moravek Biochemicals (Brea, CA). Coelenterazine was from PJK GmbH (Kleinblittersdorf, Germany). [*myo*-^{3}H]Inositol and YSi SPA beads were from GE Healthcare (Chalfont St. Giles, Buckinghamshire, UK). Glass fiber filters (GF/C) were from PerkinElmer Life and Analytical Sciences (Waltham, MA). Dulbecco's modified Eagle's medium/nutrient mixture F-12, Hanks' buffered salt solution (HBSS), trypsin-EDTA, and Hepes were from Mediatech, Inc. (Manassas, VA), pIRESHyg3 was from Clontech (Mountain View, CA), and pcDNA 3.1 was from Invitrogen (Carlsbad, CA), The AlphaScreen SureFire phospho-ERK1/2 reagents, AlphaScreen streptavidin donor beads, and anti-IgG (protein A) acceptor beads used for phosphorylated ERK1/2 detection, were purchased from PerkinElmer Life and Analytical Sciences. The pLPC retroviral vector was a generous gift from Dr. Lin Pei (Amgen Inc.). Puromycin and fatty acid-free BSA and HSA were obtained from Sigma-Aldrich (St. Louis, MO), and fetal bovine serum and hygromycin were from Invitrogen. Docosahexaenoic acid and α-linolenic acid were purchased from Sigma-Aldrich. A9 cells were obtained from American Type Culture Collection (Manassas, VA).

Cloning and Cell Culture. Full-length human FFA1 was cloned by polymerase chain reaction from human universal cDNA and subcloned into the mammalian expression vector pIRESHyg3. The aequorin DNA was subcloned into pcDNA 3.1 vector. Chinese hamster ovary (CHO) cells were stably transfected with both FFA1 and aequorin DNA. The cell line was serially diluted to obtain a monoclonal line. The double stable cell line was maintained in Dulbecco's modified Eagle's medium/nutrient mixture F-12 containing 10% fetal bovine serum, antibiotics, and hygromycin (600 μg/ml).

A stable FFA1-overexpressing cell line was generated by retroviral infection of A9 cells with full-length hFFA1 cDNA and subcloned into the pLPC retroviral vector (Lin et al., 2011). The monoclonal line was maintained in Dulbecco's modified Eagle's medium/nutrient mixture F-12 containing 10% fetal bovine serum, antibiotics, and puromycin (2 μg/ml).

The cDNA for FFAR1 was subcloned in pCMV-FLAG (Sigma-Aldrich). Mutations were made by using the site-directed mutagenesis kit from Stratagene (La Jolla, CA), and the mutated sequence was verified by sequencing.

Membrane Preparation. Membranes were isolated as described elsewhere (Swaminath et al., 2002). In brief, A9 cells expressing hFFA1 were harvested by centrifugation (10 min at 10,000*g*), washed once with phosphate-buffered saline, and recentrifuged. The pellet was resuspended in lysis buffer (10 mM Tris-HCl, pH 7.4, with 1 mM EDTA) and lysed using 30 strokes with a Dounce homogenizer. Nuclei and unbroken cells were removed by centrifugation (5 min at 500*g*). The supernatant was centrifuged, and the resulting pellet was resuspended in 20 mM lysis buffer (10 mM Tris-HCl, pH 7.5) and recentrifuged. Membranes were resuspended at 1 mg/ml protein in resuspension buffer (20 mM Hepes, pH 7.5, and 5 mM $MgCl_2$) and stored at −80°C.

Equilibrium Binding Assays. Equilibrium binding assays were performed on A9 membranes expressing hFFA1. Test compounds were diluted serially with binding buffer (20 mM Hepes, pH 7.5, 5 mM $MgCl_2$, 100 mM NaCl, and 0.1% (w/v) fatty acid-free BSA). There is a possibility of free fatty acids being present in the assays and giving the appearance of constitutive activity in the functional assays and perturbing the radioligand binding assays. Therefore, a low concentration of fatty acid-free BSA (0.1%) was included in the binding assays. Fatty acid-free BSA, up to 0.5%, had no effect on binding. The membranes and the radioligand were resuspended in the binding buffer. Each well of the 96-well assay plate contained diluted test compounds, radioligand (5 nM [^{3}H]AMG 837 or 10 nM [^{3}H]AM 1638), and A9-hFFA1 cell membrane protein (5 μg/well) in a total volume of 200 μl and was allowed to equilibrate at room temperature for 4 h. Some cross-interaction heterologous binding experiments were performed with 5 nM [^{3}H]AM 1638 and 20 μg/well membrane protein, using different concentrations of DHA in the presence or absence of different concentrations of AM 8182. The membrane protein concentration was such that not more than 10% of the added radioligand was bound to the receptor. There were 2 to 12 replicates per data point. Nonspecific binding was determined in presence of a 10 μM concentration of either AMG 837 or AM 1638, depending on the radioligand used. Plates were harvested on a GF/C filterplate with five washes of ice-cold buffer. Then 50 μl of scintillant was added to each well of the plate, and the plate was counted on a TopCount Microplate Scintillation counter (PerkinElmer Life and Analytical Sciences). All the compounds were dissolved in di-

methyl sulfoxide, which, at the highest final concentration in the assay of 1%, had no effect on binding.

Saturation Binding and Interaction Experiments. Saturation binding curves were generated using increasing concentrations (0.1–40 nM) of either the radiolabeled partial agonist [^{3}H]AMG 837 or the full agonist [^{3}H]AM 1638. The assay was performed in a 96-well plate containing either 5 μg of membrane protein for [^{3}H]AMG 837 binding or 20 μg/well for [^{3}H]AM 1638 and incubated at room temperature for 4 h. Nonspecific binding was determined in the presence of a 10 μM concentration of either unlabeled ice-cold AMG 837 or AM 1638 as appropriate. Saturation interaction experiments were performed in the presence of 100 nM AM 1638 (for [^{3}H]AMG 837 binding curves) or 100 nM AMG 837 (for [^{3}H]AM 1638). The binding reactions were terminated, and radioactivity was measured as described above. Saturation curves were generated using 3 to 12 replicates for each data point. Not more than 10% of added radioligand was bound to the receptor at any radioligand concentration.

Dissociation Binding Kinetics. The dissociation rate of [^{3}H]AMG 837 from the FFA1 receptor was measured in the absence or presence of a range of concentrations of agonist (AM 1638 or AM 8182). The assay plate containing membrane protein (5 μg) and 5 nM [^{3}H]AMG 837 was preequilibrated for 2 h at room temperature (shaking at 230 rpm). At time 0, total binding was determined, and saturating amounts of ice-cold AMG 837 (10 μM), in the presence or absence of different concentrations of allosteric ligand were added to the different wells of the plate containing the prelabeled membranes. The membranes were filtered at different times (2–240 min) followed by five washes with cold buffer, and radioactivity was measured as described above.

Aequorin Assay. CHO cells stably expressing both FFA1 and aequorin DNA were grown in 15-cm dishes, harvested 24 h later using 2 ml of 1× trypsin-EDTA (0.25% trypsin and 21 mM EDTA in Hanks' buffered salt solution) and pelleted by centrifugation (5 min, 600*g*). The pellet was resuspended in HBSS containing 0.01% (w/v) fatty acid-free HSA and 20 mM Hepes and incubated with 1 μg/ml coelenterazine and test compounds at room temperature for 2 h. Aequorin luminescence measurements as a readout for ligand-induced receptor activation and calcium release were made using a 96-well luminometer (Berthold Technologies, Bad Wildbad, Germany). The response was measured over a 20-s interval after addition of compounds to the cells (An et al., 1998).

This stable cell line expressed low levels of FFA1 relative to those for the A9 cells. The best estimate of the B_{max} levels, obtained from the measurement of [^{3}H]AMG 837 (1 nM) binding to membranes (10 μg of protein) prepared in the same way as the A9 membranes, is approximately 0.5 pmol/mg protein, assuming that the affinity of AMG 837 is the same as that measured in A9 membranes. Specific binding of [^{3}H]AM 1638 (5 or 10 nM) to CHO cell membranes could not be detected (data not shown).

CHO-KI cells (2×10^6 cells/dish) for transient transfections were seeded in 145-mm dishes and cultured with media containing Dulbecco's modified Eagle's medium/nutrient mixture F-12 and 10% fetal bovine serum. The cells were incubated at 37°C with 5% CO_2 overnight and transfected with 10 μg of pCMV-FLAG with wild-type FFAR1 or the FFAR1 mutants and 10 μg of pcDNA 3.1 aequorin vector constructs on the following day. Twenty-four hours after transfection, the cells were detached in phosphate-buffered saline containing 1 mM EDTA, loaded with coelentrazine, and assayed as described above.

FACS Analysis. CHO-K1 cells were seeded in six-well Falcon Primaria plates (BD, Franklin Lakes, NJ) at a density of 250,000 cells/well and incubated overnight at 37°C and 5% CO_2. On the next day, the cells were transfected with 2.5 μg of FLAG-tagged wild-type or mutant constructs using Lipofectamine 2000 (Invitrogen) according to the manufacturer's protocol. The cells were harvested with phosphate-buffered saline containing 2 mM EDTA, and the pellet was gently resuspended in 100 μl of primary antibody staining solution using a monoclonal anti-FLAG M2 antibody (Sigma-Aldrich) or mouse IgG (MOPC21) isotype control (Sigma-Aldrich) at 10 μg/ml in ice-cold FACS buffer (phosphate-buffered saline with 2 mM EDTA and 2% fetal bovine serum). Primary antibody staining was performed on ice for 45 min, followed by two washes with phosphate-buffered saline with 2 mM EDTA.

Secondary antibody staining was performed in 100 μl/reaction FACS buffer containing a polyclonal goat anti-mouse F(ab′)$_2$ fragment conjugated to fluorescein isothiocyanate (Dako North America, Inc., Carpinteria, CA) at 40 μg/ml on ice for 45 min followed by three washes. The cells were resuspended in 0.5 ml of FACS buffer and analyzed using a Cytomics FC500 FACS analyzer (Beckman Coulter, Fullerton, CA). Geometric mean values of anti-FLAG stained samples were analyzed and compared with the corresponding mouse IgG isotype sample controls.

Inositol Phosphate Accumulation Assay. A9 is a murine fibroblast cell line derived from the L-cell line (Allderdice et al., 1973). A9 cells stably expressing FFA1 receptor were seeded in a 96-well plate (25,000 cells/well) and labeled with [*myo*-^{3}H]inositol for 16 h (overnight). The cells were then treated for 1 h at 37°C with serial dilutions of test compounds in HBSS containing 25 mM Hepes (pH 7.4), 10 mM LiCl, and 0.01% (w/v) HSA. Cells were lysed with 20 mM formic acid for 4 h at 4°C. YSi SPA beads were added to the cell lysates and incubated overnight in the dark. Radioactivity was recorded on a MicroBeta scintillation counter (PerkinElmer Life and Analytical Sciences).

ERK Phosphorylation Assay. A9 cells expressing the FFA1 receptor were seeded in 96-well poly-D-lysine plates (25,000 cells/well) and cultured overnight in culture media (Dulbecco's modified Eagle's medium-F12, 1% penicillin/streptomycin, 1% L-glutamine, and 10% (v/v) fetal bovine serum). The following day, cells were cultured overnight in serum-free media containing 0.1% (w/v) BSA. For the agonist-stimulated response, cells were incubated with fresh serum-starved media at 37°C in presence of compounds for 15 min. The reaction was terminated by removal of the media containing the compounds and lysed with 100 μl of 1× lysis buffer from the SureFire kit. All the subsequent steps were followed according to the manufacturer's protocol. Allosteric interaction experiments were conducted at varying concentrations of agonist in the presence of fixed concentrations of the allosteric modulator.

Isolation of Pancreatic Islets and Insulin Secretion Measurements. Pancreatic islets of Langerhans were isolated from wild-type (C57BL/6) mice by collagenase digestion. The islets were cultured overnight in regular islet media (RPMI 1640 medium containing 11.5 mM glucose and 10% (v/v) fetal calf serum with supplements) to facilitate recovery from the isolation process. Insulin secretion was determined by a 1-h static incubation in Krebs-Ringer-bicarbonate buffer in a 96-well format as described previously (Herrington et al., 2006). In brief, the islets in the 96-well plates (two islets size-matched/well) were preincubated in Krebs-Ringer-bicarbonate with 2 mM glucose and 0.1% (w/v) HSA for 1 h. This was followed by treatment with compounds for 1 h. Insulin secretion was determined in the supernatant using the ultrasensitive mouse insulin enzyme-linked immunosorbent assay kit (ALPCO Diagnostics, Salem, NH).

Oral Glucose Tolerance Test. Streptozotocin (STZ) is an antibiotic that causes pancreatic β-cell destruction, insulin deficiency, and hyperglycemia. This model is frequently used for evaluating the efficacy of compounds in vivo for type 2 diabetes (Tahara et al., 2011). High-fat STZ-treated mice were fasted overnight, and compounds were orally administered the following morning. Glucose load (2 g/kg) was given orally at 60 min after compound treatment. Blood samples were taken from the tail at −60, 0, 15, 30, 60, and 120 min. The plasma was separated by centrifugation at 10,000*g* for 6 min at 4°C. Plasma glucose was measured using a calorimetric assay kit obtained from Wako Chemicals USA, Inc. (Richmond, VA). Plasma insulin was measured using a rat insulin enzyme-linked immunosorbent assay kit (ALPCO Diagnostics). Compounds were prepared as a

suspension in 1% Tween 80 and 1% methylcellulose and administered orally (10 ml/kg).

Miscellaneous. Protein was determined using the DC protein assay kit (Bio-Rad Laboratories, Hercules, CA).

Data Analysis. All the results are in general presented as means ± S.E.M. of at least three independent experiments. Data were analyzed with nonlinear regression analysis using Prism 5.01 (GraphPad Software Inc., San Diego, CA) and its library equations to analyze saturation binding curves, dose-response curves, and Gaddum-Schild analysis.

Simple allosteric binding interactions (both equilibrium and dissociation kinetics) were analyzed using equations derived from the allosteric ternary complex model (Lazareno and Birdsall, 1995). These analyses, in the case of equilibrium data, provided estimates of the affinities of the allosteric ligand for the unoccupied receptor (K_X) and the binding cooperativity, α, between the allosteric ligand (X) and the radioligand (L), where $\text{Bound}_{L,X}$ is the specific bound radioligand in the presence of X and $\text{Bound}_{L,X=0}$ is the specifically bound radioligand in the absence of X (eq. 1). The affinity of X for the radioligand-occupied receptor (i.e., in the ternary complex) is $\alpha \cdot K_X$:

$$\text{Bound}_{L,X} = \text{Bound}_{L,X=0}\frac{(1 + K_L[L])(1 + \alpha \cdot K_X[X])}{(1 + K_X[X] + K_L[L](1 + \alpha \cdot K_X[X]))} \quad (1)$$

In the case of the dissociation data, the affinity of the allosteric ligand for the radioligand-occupied receptor was estimated from the midpoint of the plot of the observed dissociation rate constant k_{obs} against the log[allosteric ligand]. This value should be close to (within a factor of 2–3: Lazareno and Birdsall, 1995) and theoretically identical to the value obtained from equilibrium experiments if the allosteric ternary complex model is an appropriate model to analyze the data.

Functional data were in general normalized to the maximum response given by a full agonist. The aequorin and IP accumulation assay interaction data were analyzed using the following equation derived from the operational model of allosteric interactions (Leach et al., 2007). This simplified equation, shown below (eq. 2), is based on the assumption that one of the agonists, A, is a full agonist in this system; i.e., it has a value of τ_A that is much greater than 1 [the τ value of a ligand denotes its capacity to exhibit agonism and incorporates its intrinsic efficacy, the density of receptors, and the efficiency of stimulus-response coupling (Black and Leff, 1983)].

$$E = \text{Basal} + E_{max}\frac{\{[A](1+\alpha\cdot\beta\cdot K_B\cdot[B]+\tau_B\cdot \text{EC}_{50,A}\cdot K_B\cdot[B])\}^n}{\{\text{EC}_{50,A}(1 + K_B\cdot[B])\}^n + \{[A](1 + \alpha\cdot\beta\cdot K_B\cdot[B] + \tau_B\cdot \text{EC}_{50,A}\cdot K_B\cdot[B])\}^n} \quad (2)$$

where A is a full agonist, B is a partial agonist (e.g., AMG 837) that binds allosterically with A, α is a cooperativity factor for the modulation of affinity, β is a cooperativity factor for the modulation of efficacy, K_B is the affinity constant of the allosteric ligand, EC_{50} is the potency of A, τ_B is the τ value for the partial agonist B, E is the response, E_{max} is the maximum response above basal activity, basal is basal activity, and n is the slope factor describing the dose-response curves of the full agonist, A. This equation provides values of the composite parameter, $\alpha\beta$, the overall cooperativity factor for the combined change in agonist potency and efficacy due to the agonists forming and activating the ternary complex. For the data analyses [A], [B], $\text{EC}_{50,A}$, K_A, $\alpha\beta$, and τ_B are all expressed as log values, and the equation was amended accordingly. Dose-response curves of A are plotted at different fixed concentrations of B (title of the data columns). The value of β, the change in stimulus to the system provided by A and B in the presence of the other ligand, can be estimated by dividing $\alpha\beta$ by the cooperativity value found in binding studies.

A minor rearrangement to eq. 3 was used to analyze the interaction data, where the dose-response curves of the partial agonist (now called A, affinity K_A, and efficacy τ_A) are measured at different fixed concentrations of the full agonist (now called B, $\text{EC}_{50,B}$). n is now the slope factor of the partial agonist, B:

$$E = \text{Basal} + E_{max}\frac{\{[B](1 + \alpha\cdot\beta\cdot K_A\cdot[A] + \tau_A\cdot \text{EC}_{50,B}\cdot K_A\cdot[A])\}^n}{\{\text{EC}_{50,B}(1 + K_A\cdot[A])\}^n + \{[B](1+\alpha\cdot\beta\cdot K_A\cdot[A]+\tau_A\cdot\text{EC}_{50,B}\cdot K_A\cdot[A])\}^n} \quad (3)$$

Potencies, affinities, and cooperativities are expressed as log values ± S.E.M. (n). In the very small number of examples where n = 2, the data are expressed as means ± range/2.

Results

Activation of the FFA1 Receptor by Synthetic and Endogenous Agonists in Different In Vitro Assays. The novel synthetic agonists for FFA1 receptor were identified after a high-throughput screen and subsequent development of detailed structure-activity relationships (SARs) from selected hits. The specificity of all the synthetic ligands, up to concentrations of 30 μM, was checked by screening against several GPCRs in a panel that included the FFA2, FFA3, GPR119, and glucagon-like peptide 1 receptors. The chemical structures of the synthetic ligands used in the assays reported here are depicted in Fig. 1 together with, for comparison purposes, those of DHA and α-linolenic acid (LA).

DHA is one of the endogenous ligands for the FFA1 receptor (Briscoe et al., 2003). We therefore looked at the activity of the novel synthetic agonists (AMG 837, AM 8182, and AM 1638) in various functional assays and compared their potencies and efficacies relative to those of DHA. A more limited series of experiments were performed on AM 6331 (Supplemental Figs. 1 and 2), an agonist closely related in structure to AMG 837 (Fig. 1).

Because it is been shown that FFA1 couples primarily to $G\alpha_q$ and elicits a calcium response (Briscoe et al., 2003), aequorin assays were performed to look at the activation of receptor by the synthetic ligands. The assay was performed on a CHO cell line expressing low levels of the FFA1 receptor (approximately 0.5 pmol/mg protein; see *Materials and Methods*). The synthetic agonists AM 1638 and AM 8182 were full agonists compared with DHA, but AMG 837 was a partial agonist with approximately 30% of the E_{max} of the full agonists (Fig. 2A). The synthetic agonists, AMG 837 and AM 1638, were 400- to 500-fold more potent than DHA (Table 1), which had an EC_{50} of ~40 μM in this assay. AM 8182 was approximately 15-fold more potent than DHA.

To confirm that the synthetic agonists AM 8182 and AM 1638 are indeed full agonists and that AMG 837 has a lower E_{max}, we performed IP accumulation assays on transfected A9 cells stably expressing the FFA1 receptor in the range of 6 to 9 pmol/mg protein. In this cell line the E_{max} values of AM 1638 and AM 8182 were similar and comparable to that of DHA (Fig. 2B). Even at the high levels of receptor expression, the E_{max} value of AMG 837, somewhat surprisingly, was only 50% of that of the synthetic full agonists and DHA, indicating that it is indeed a partial agonist (Fig. 2B). All the ligands were more potent (10–40-fold) in this assay relative to the aequorin assay, even the partial agonist AMG 837 (Table 1). However, as observed in the aequorin assay, the synthetic agonists were more potent than DHA (15–1500-fold) with AMG 837 and AM 1638 being active at low nanomolar con-

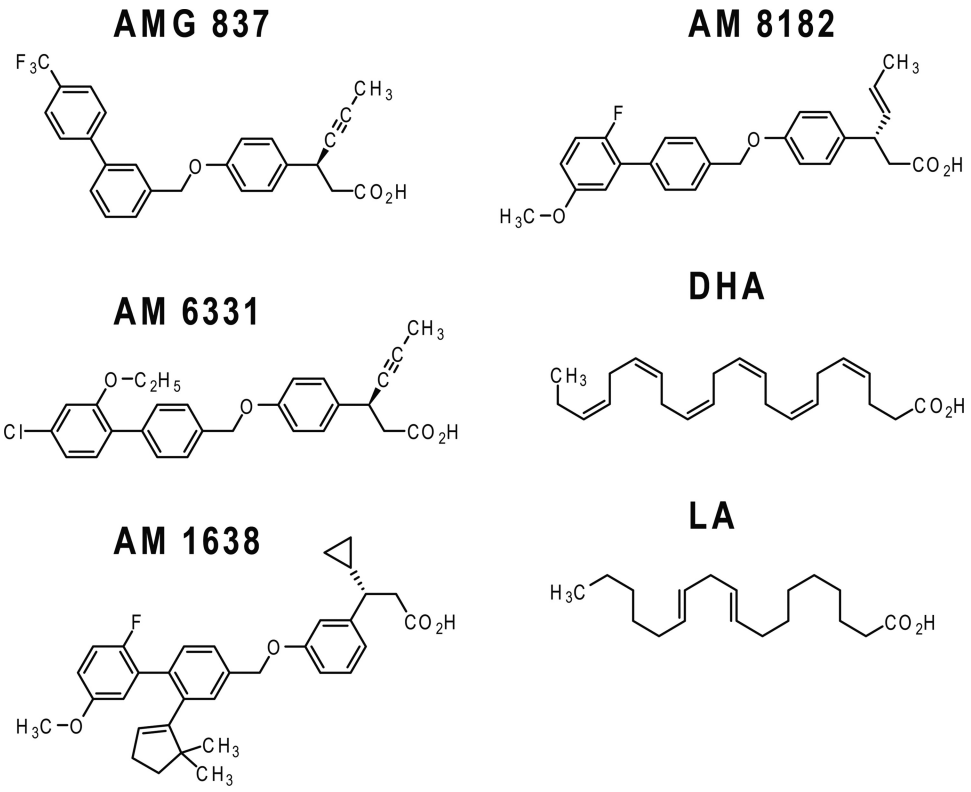

Fig. 1. Chemical structures of novel allosteric agonists and endogenous ligands of the FFA1 receptor.

centrations. AM 6331 was less potent than AMG 837 and also a partial agonist, exhibiting efficacy comparable to that of AMG 837.

It is well established that the activation of G protein-coupled receptors induces a mitogen-activated protein kinase signal transduction cascade. We therefore examined the induction of ERK phosphorylation by agonist-mediated activation of FFA1 in the A9 cell line (Fig. 2C; Table 1). The synthetic agonists, AM 1638 and AM 8182, gave the same E_{max} values as DHA, an effect observed in the other in vitro functional assays. In contrast AMG 837 was again a partial agonist in this assay, exhibiting 30% of the E_{max} of DHA (Fig. 2C). The agonists were most potent in the IP accumulation assay on the higher expressing A9 cell line and weakest in the aequorin assay on the lower expressing CHO cell line. In general, the rank order of potency and efficacy of the agonists was similar in the three assays.

Binding of Radioligands to the FFA1 Receptor. The lower-efficacy agonist, AMG 837, and the high-efficacy agonist, AM 1638, were both radiolabeled with tritium, and saturation curves of their binding to A9 membranes transfected with the FFA1 receptor were measured. The binding curves for both [^{3}H]AMG 837 and [^{3}H]AM 1638 were well described by simple binding isotherms (slope factor = 1 as illustrated in Fig. 5, A and B). The mean log affinities of [^{3}H]AMG 837 and [^{3}H]AM 1638 were 8.44 ± 0.05 (K_d = 3.6 nM, n = 7) and 7.87 ± 0.03 (K_d = 13 nM, n = 6), respectively. In experiments on the same membrane preparation and at the same protein concentration, the B_{max} values of [^{3}H]AMG 837 and [^{3}H]AM 1638 were 7.9 ± 0.5 pmol/mg protein (n = 3) and 8.4 ± 0.7 pmol/mg protein (n = 3), respectively. There was no significant difference in the B_{max} values of the two radioligands (unpaired t test).

Equilibrium Binding Assays of the Interaction of the Synthetic Ligands and DHA with the Radiolabeled FFA1 Receptor. The ability of AMG 837, AM 1638, AM 8182, and DHA to modulate 5 nM [^{3}H]AMG 837 binding was examined (Fig. 3). As expected, AMG 837 fully inhibited specific [^{3}H]AMG 837 binding with a mean pIC_{50} of 8.13 ± 0.06 (n = 4), a value compatible with the K_d value measured in the saturation experiments.

Most unexpectedly, however, AM 1638 strongly enhanced the binding of [^{3}H]AMG 837. The data, when analyzed by the allosteric ternary complex model, gave a log affinity of AM 1638 for the unoccupied FFA1 receptor of 7.58 ± 0.07 (n = 6), a value similar to the value found in the direct saturation experiment. The estimate of the log affinity of AM 1638 for the [^{3}H]AMG 837-occupied receptor was 8.14 ± 0.10 (n = 6), indicating that the data are compatible with a 3.6-fold positive cooperativity between AM 1638 and AMG 837. In contrast with AM 1638, AM 8182 and DHA both inhibited [^{3}H]AMG 837 binding (Fig. 3) but not competitively because the inhibition curves did not extrapolate to zero specific binding at high concentrations. These data were analyzed using the allosteric ternary complex model to give a log affinity of 6.04 ± 0.08 (n = 4) for AM 8182 at the unoccupied receptor and 28 ± 5-fold negative cooperativity with [^{3}H]AMG 837. Likewise, DHA had a log affinity of 5.33 ± 0.03 (n = 6) at the unoccupied receptor and 9.8 ± 0.5-fold negative cooperativity with [^{3}H]AMG 837. These results show that AM 1638, AM 8182, and DHA do not bind to the same site as AMG 837. There was no detectable effect of guanosine 5′-*O*-(3-thio) triphosphate (10 μM) on the binding of [^{3}H]AMG 837 or on the enhancing ability of AM 1638 (data not shown).

Analogous cross-interaction binding experiments were performed using [^{3}H]AM 1638 as the radioligand (Fig. 4). As

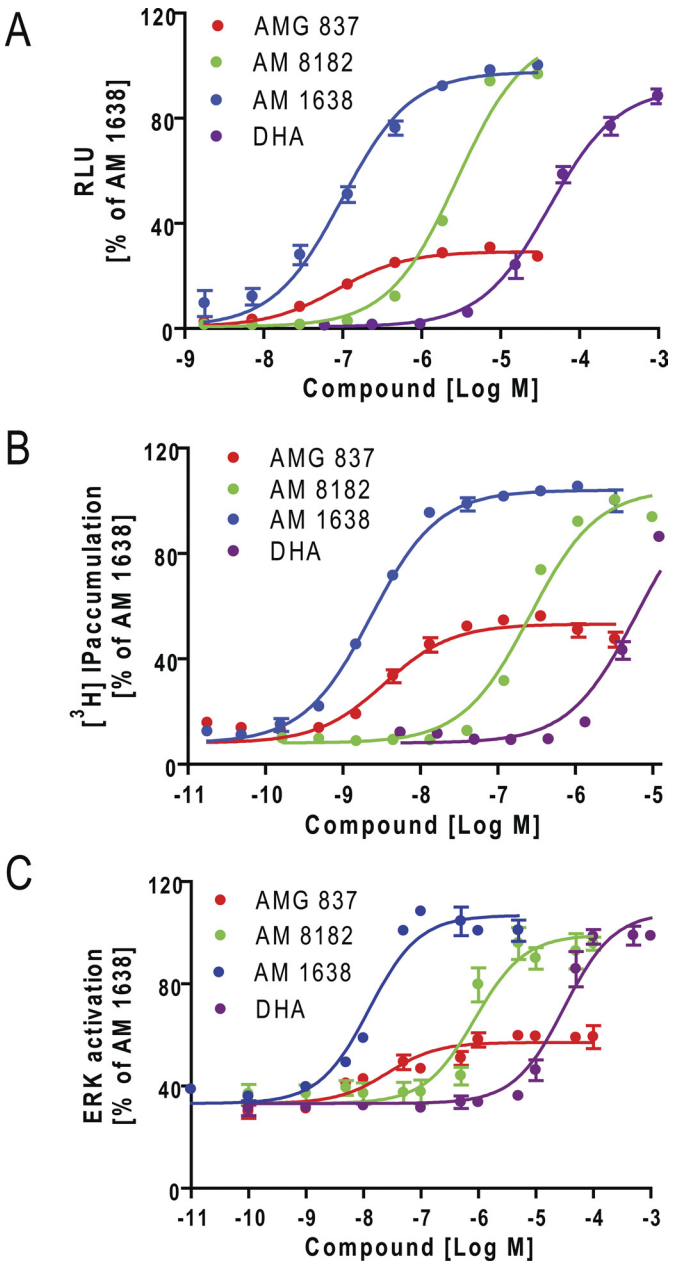

Fig. 2. Activation of the FFA1 receptor by synthetic agonists and the endogenous ligand DHA. Dose-response curves for the four agonists shown in the figure were generated using three assays: induced [Ca^{2+}] release, recorded as the aequorin luminescence signal (A); activation of IP accumulation in A9 cells expressing hFFA1 receptor (B); and stimulation of the ERK pathway by FFA1 agonists in A9 cells expressing the hFFA1 (C). Data are expressed as a percentage of the control maximal response of the full agonist AM 1638 and are shown as the means ± S.E.M. of three to six experiments performed in duplicate or triplicate. The data were fitted using a dose-response equation with the slope factors constrained to 1. The mean parameters of these and other individual experiments are shown in Table 1. RLU, relative luminescence units.

TABLE 1
Functional potencies of the FFA1 agonists

Compound	−Log EC_{50} ± S.E.M. (*n*)		
	Aequorin	IP Accumulation	ERK
AMG 837	7.06 ± 0.11 (11) E_{max} 30 ± 3%	8.46 ± 0.08 (6) E_{max} 50 ± 2%	7.58 ± 0.25 (4) E_{max} 30 ± 4%
AM 8182[a]	5.55 ± 0.04 (12)	6.59 ± 0.04 (6)	6.06 ± 0.09 (6)
AM 1638[a]	7.01 ± 0.04 (9)	8.64 ± 0.04 (6)	7.90 ± 0.13 (2)
DHA[a]	4.38 ± 0.11 (10)	5.22 ± 0.10 (6)	4.51 ± 0.11 (4)
AM 6331[b]	6.28 ± 0.10 (8)	6.71 ± 0.05 (2)	N.D.

[a] Full agonists.
[b] E_{max} not significantly different from that of AMG 837.

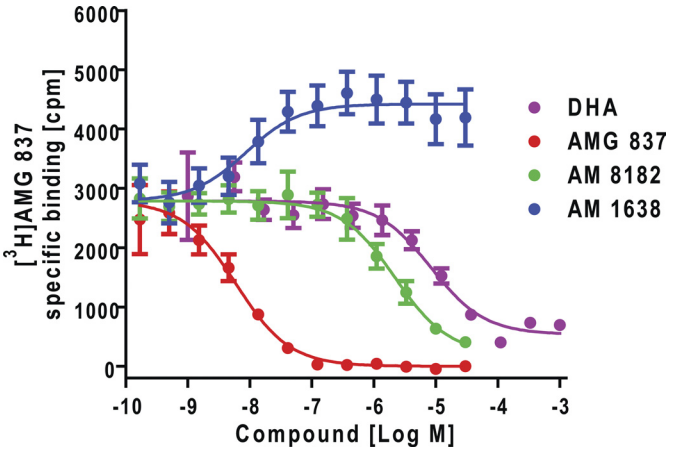

Fig. 3. The effects of AMG 837, AM 8182, DHA, and AM 1638 on the binding of [^{3}H]AMG 837 at the human FFA1 receptor. Data are expressed as counts per minute specific binding and are shown as means ± S.E.M. of two to three independent experiments performed in duplicate. The curves represent the best fit of a competitive model for AMG 837 and the allosteric ternary complex model for other agonists. The mean log affinity parameters from the analyses of these and replicate experiments are shown in Table 2. The log cooperativities are reported in Table 3.

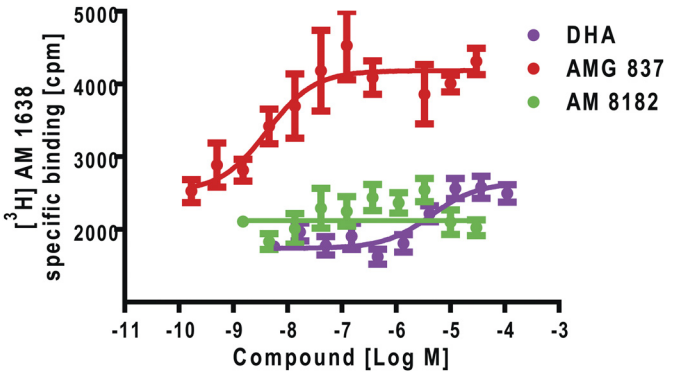

Fig. 4. The effects of AMG 837, AM 8182, and DHA on the binding of [^{3}H]AM 1638 to the human FFA1 receptor. Data points represent the means ± S.E.M. of three independent experiments, with duplicate replicates. The curves represent fits of the data to the allosteric ternary complex model, except for that of AM 8182, for which a horizontal line is shown to indicate a total lack of interaction in equilibrium binding. The mean log affinities and cooperativities from the analysis of these and other experiments are reported in Tables 2 and 3, respectively. The best-fit curves start at slightly different levels because each curve had its own data points representing binding in the absence of interacting ligand.

would be predicted by the interpretation of the data in Fig. 3 using the allosteric ternary complex model, AMG 837 considerably enhanced the binding of 10 nM [^{3}H]AM 1638. The estimated mean log affinity of AMG 837 for the unoccupied receptor was 8.34 ± 0.14 (n = 8) which, as expected, agreed with the value (8.44) found in the saturation experiments. The calculated positive cooperativity was 2.5 ± 0.4-fold (n = 8) and was also in reasonable agreement with that found in the [^{3}H]AMG 837-AM 1638 interaction experiments. The reciprocal magnitude and the nature of the cooperative interaction between AMG 837 and AM 1638 were thus confirmed using radioligands that labeled the two different binding sites. The homologous inhibition curves for AM 1638 gave

TABLE 2
Binding affinity constant of the FFA1 agonists

Compound	Log$K$ ± S.E.M. (n)
AMG 837	8.44 ± 0.05 (7)[a]
	8.34 ± 0.14 (8)[b]
AM 1638	7.87 ± 0.03 (6)[a]
	7.58 ± 0.07 (6)[c]
AM 8182	6.04 ± 0.08 (4)[c]
DHA	5.33 ± 0.03 (6)[c]
	5.19 ± 0.14 (6)[b]
AM 6331	8.26 ± 0.03 (4)[c]

[a] From saturation experiments.
[b] From interaction experiments with [^{3}H]AM 1638.
[c] From interaction experiments with [^{3}H]AMG 837.

a pIC_{50} of (7.91), which has a relatively large error associated with it (±0.12, $n = 5$) but is compatible with the log affinity value obtained from the saturation curves (Table 2).

The mutual enhancing effects of AMG 837 and AM 1638 on each other's binding were further explored by generating saturation curves of 1) [^{3}H]AMG 837 in the presence and absence of AM 1638 (100 nM) and 2) of [^{3}H]AM 1638 in the presence and absence of AMG 837 (100 nM). The concentrations of unlabeled ligands were chosen to be those at which close to maximal effects on the binding of the heterologous radioligand were observed (see Figs. 3 and 4). Figure 5C shows that the log affinity of [^{3}H]AMG 837 increased from 8.48 ± 0.07 to 8.77 ± 0.06 ($n = 4$) (a 2-fold increase) in the presence of AM 1638. Likewise, the log affinity of [^{3}H]AM 1638 increased from 7.87 ± 0.03 to 8.20 ± 0.02 ($n = 4$), a 2.3-fold increase in the presence of AMG 837 (Fig. 5D).

In both sets of saturation curves, there was no significant change in B_{max} in the single experiment illustrated in Fig. 5 and in replicate experiments. The mean ratios of the B_{max} values for [^{3}H]AMG 837 and [^{3}H]AM 1638 in the presence and absence of the other nonradioactive ligand were 1.00 ± 0.07 ($n = 4$) and 1.06 ± 0.07 ($n = 6$), respectively. Therefore, the increases in radioligand binding seen in Figs. 3 and 4 are solely due to increases in affinity and not to an increase in B_{max}.

In contrast with the negatively cooperative interaction between both DHA and AM 8182 with [^{3}H]AMG 837, AM 8182 had no detectable significant reproducible effect on [^{3}H]AM 1638 binding and DHA had a slightly positively cooperative interaction (2.2 ± 0.2-fold, $n = 6$) (Fig. 4; Tables 2 and 3) with the estimated mean log affinity of DHA for the unoccupied receptor (5.19 ± 0.14) agreeing with that found in the [^{3}H]AMG 837-DHA interaction experiments (5.33).

The equilibrium interaction assays show that AM 1638 and AMG 837 bind to different distinct sites on the receptor in a reciprocal cooperative fashion and that both AM 8182 and DHA bind allosterically with both AMG 837 and AM 1638. The interaction between AM 8182 and DHA was explored further by examining how the enhancement of [^{3}H]AM 1638 binding by DHA, illustrated in Fig. 4, was modified by increasing concentrations of AM 8182 (1–10 μM) (Fig. 6). Because AM 8182 has no effect on [^{3}H]AM 1638 binding (Fig. 4), if AM 8182 and DHA are interacting competitively, then AM 8182 should shift the DHA enhancement curve in a parallel fashion. The data in Fig. 6 and from four replicate experiments were well fitted by the Gaddum-Schild equation. The mean pA_2 value for AM 8182 is 6.24 ± 0.10 ($n = 5$), which agrees with the value shown in Fig. 3 and Table 2. The log affinity of DHA (5.18 ± 0.08) for the unoccupied receptor and

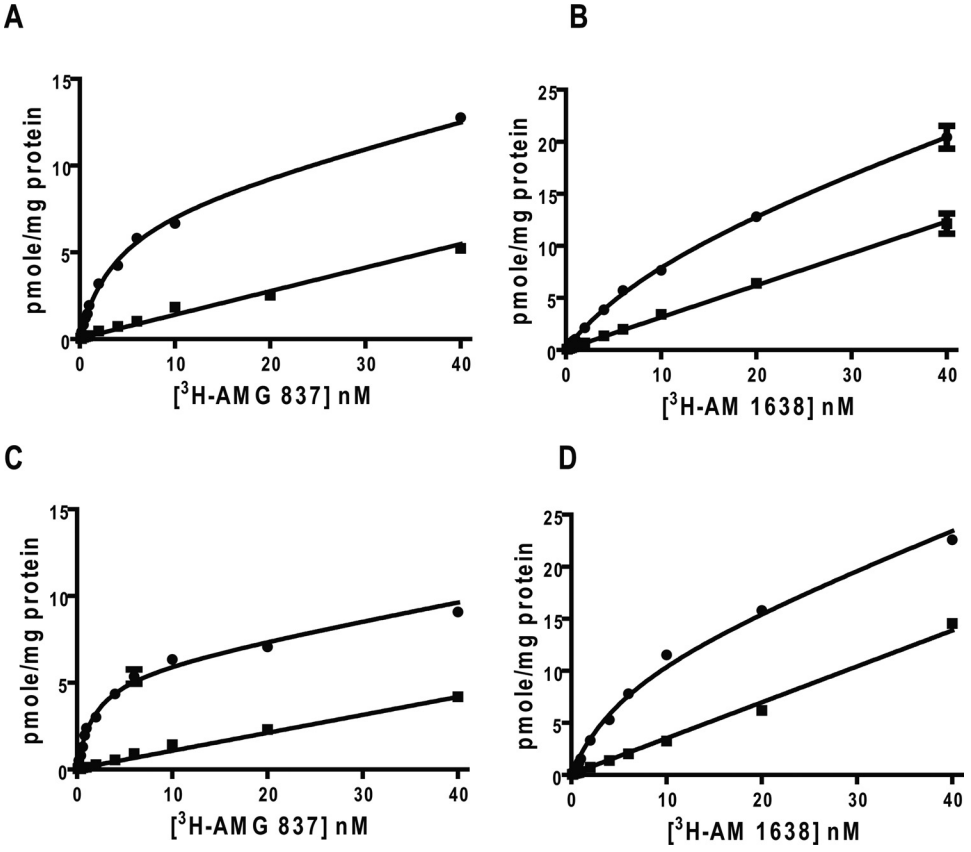

Fig. 5. Saturation binding curves of [^{3}H]AMG 837 and [^{3}H]AM 1638 to the human FFA1 receptor measured in the absence and presence of the heterologous ligand. Saturation curves for [^{3}H]AMG 837 and [^{3}H]AM 1638 in the absence of heterologous ligand are shown in A and B, respectively. Total binding (●) and nonspecific binding (■) are shown. Cross-interaction studies were conducted in presence of 100 nM AM 1638 for [^{3}H]AMG 837 saturation binding (C) or with 100 nM AMG 837 for [^{3}H]AM 1638 saturation binding (D). The data are from a single experiment, representative of four to six independent experiments conducted in duplicate. The curves were fitted using an equation for a single binding site and linear nonspecific binding. The mean log affinities are reported in Table 2.

TABLE 3
Cooperative interactions in binding assays

Compound	Log Cooperativity ± S.E.M. (*n*)			
	AMG 837	AM 1638	AM 8182	DHA
[^{3}H]AMG 837	—[a]	0.29 ± 0.09 (2)[b]		
	—	0.56 ± 0.12 (3)[c]	−1.45 ± 0.07 (3)[c]	−0.99 ± 0.03 (3)[c]
		0.66 ± 0.10 (6)[d]	−0.96 ± 0.18 (6)[d]	
[^{3}H]AM 1638	0.33 ± 0.04 (3)[b]	—	0.05 ± 0.03 (3)[c,e]	0.34 ± 0.04 (3)
	0.40 ± 0.05 (4)[c]	—		

[a] Homologous inhibition experiments; no cooperative interactions.
[b] From saturation experiments.
[c] From equilibrium experiments.
[d] From dissociation kinetics.
[e] Essentially neutral cooperativity; no significant effect on equilibrium binding -log affinity of the unoccupied receptor fixed at 6.04.

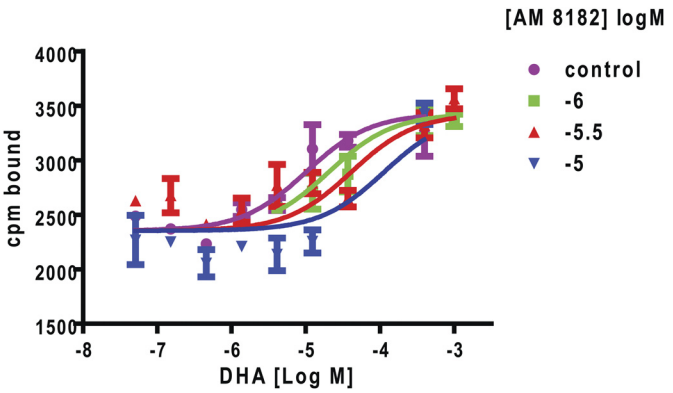

Fig. 6. Apparent competitive interaction between DHA and AM 8182 at the FFA1 receptor. [^{3}H]AM 1638 interaction binding studies were conducted using different concentrations of DHA in the presence of fixed concentrations of AM 8182. Data are expressed as specific binding (counts per minute) and are from a representative experiment from five independent experiments conducted in hextuplicate. The data were fitted using the Gaddum-Schild equation, assuming that AM 8182 has no effect on the equilibrium binding of [^{3}H]AM 1638. The mean data for the parameters derived from these experiments are reported in the text.

its cooperativity with [^{3}H]AM 1638 (2–2.5-fold) agree with those reported in Tables 2 and 3.

Effects of AM 8182 and AM 1638 on the Dissociation Kinetics of [^{3}H]AMG 837. The dissociation of [^{3}H]AMG 837 from its binding site on the FFA1 receptor appeared to be monoexponential with a k_{off} of 0.036 ± 0.002 min^{-1} ($t_{1/2}$ = 19 min, n = 8) (Fig. 7, A and B). Increasing concentrations of AM 1638 progressively slowed the rate of dissociation of AMG 837 (Fig. 7A) with an estimated log affinity of 8.51 ± 0.06 (n = 4) of AM 1638 for the [^{3}H]AMG 837-occupied receptor and a maximum approximately 4-fold slowing of dissociation being observed at concentrations of AM 1638 greater than 100 nM (Fig. 7A, inset). This log affinity value agrees reasonably with the log affinity of AM 1638 for the [^{3}H]AMG 837-occupied receptor obtained from the equilibrium and saturation binding data, as would be predicted by the allosteric ternary complex model. At all concentrations of AM 1638, the dissociation curves for [^{3}H]AMG 837 approximated closely to monoexponential decays.

The allosteric interaction of AM 8182 with AMG 837 was also explored in dissociation kinetic assays (Fig. 7B). Up to the maximum concentration that could be examined (10 μM), AM 8182 progressively decreased [^{3}H]AMG 837 dissociation. The estimated log affinity of AM 8182 for the [^{3}H]AMG 837-occupied receptor was 5.1 ± 0.2 (n = 6), assuming an allosteric ternary complex model in which high concentrations of AM 8182 will completely inhibit [^{3}H]AMG 837 dissociation. This value is in reasonable agreement with the equivalent value (4.6) calculated from the equilibrium data.

Partial Agonist AMG 837 Is Allosteric with the Full Agonists AM 8182 and AM 1638 in Functional Assays. As shown in Fig. 2 the synthetic agonists and DHA behave as agonists in various in vitro functional assays. Given the differences in their chemical structure and their allosteric binding interactions at the receptor, we were interested to see how these effects would be translated in our in vitro functional assays. To address this question, the activation of synthetic full agonists, AM 8182 or AM 1638, in presence of various concentrations of AMG 837, was measured in the aequorin, inositol phosphate accumulation, and ERK assays.

Although AM 8182 displays negative cooperativity with AMG 837 in equilibrium binding assays (α = ~0.1), we observe positive cooperativity with AMG 837 in the Ca^{2+} (aequorin), ERK, and IP accumulation functional assays (Fig. 8, A–C). The cooperativity can be seen clearly in the enhanced responses of AMG 837 to threshold concentrations of AM 8182. The data were analyzed using the operational version of the allosteric ternary complex model that takes account of the efficacies of the agonists and any change in efficacy of the ternary complex and the slope of the dose-response curves (Leach et al., 2007). The best fit curves in Fig. 8, A–C, show the excellent fit to the model with the best-fit parameters given in the figure legends. The functional cooperativity factors are in the range of 2.9 to 3.6, with the high values of β reflecting the very large increase in efficacy (26–33-fold) of each ligand in the ternary complex, AMG 837-receptor-AM 8182, relative to those observed in the binary complexes. It should be noted that in this series of experiments, the dose-response curves for AM 8182 are steep, with slope factors of 1.5 to 2. Indeed, the slope factors for AM 8182 are somewhat greater than 1 in Fig. 2. AM 8182 is not a potent ligand, and it is relatively insoluble. The steep slope may be due to insolubility or to a nonspecific effect at the highest concentrations.

In conjunction with the in vitro results in transfected cells, AMG 837 acted as a partial agonist in stimulating insulin secretion approximately 2.5-fold in the more relevant physiological settings of the mouse islet cell preparation (Fig. 9A) with the log potency (−6.6 ± 0.5, n = 4). This stimulation is less than the 4-fold stimulation given by a submaximal dose of AM 8182. The response of AMG 837 was strongly enhanced in the presence of threshold or subthreshold concentrations of AM 8182. A functional positive cooperativity factor of 7 ± 2 was estimated when the data were analyzed by the operational version of the allosteric ternary complex model. The

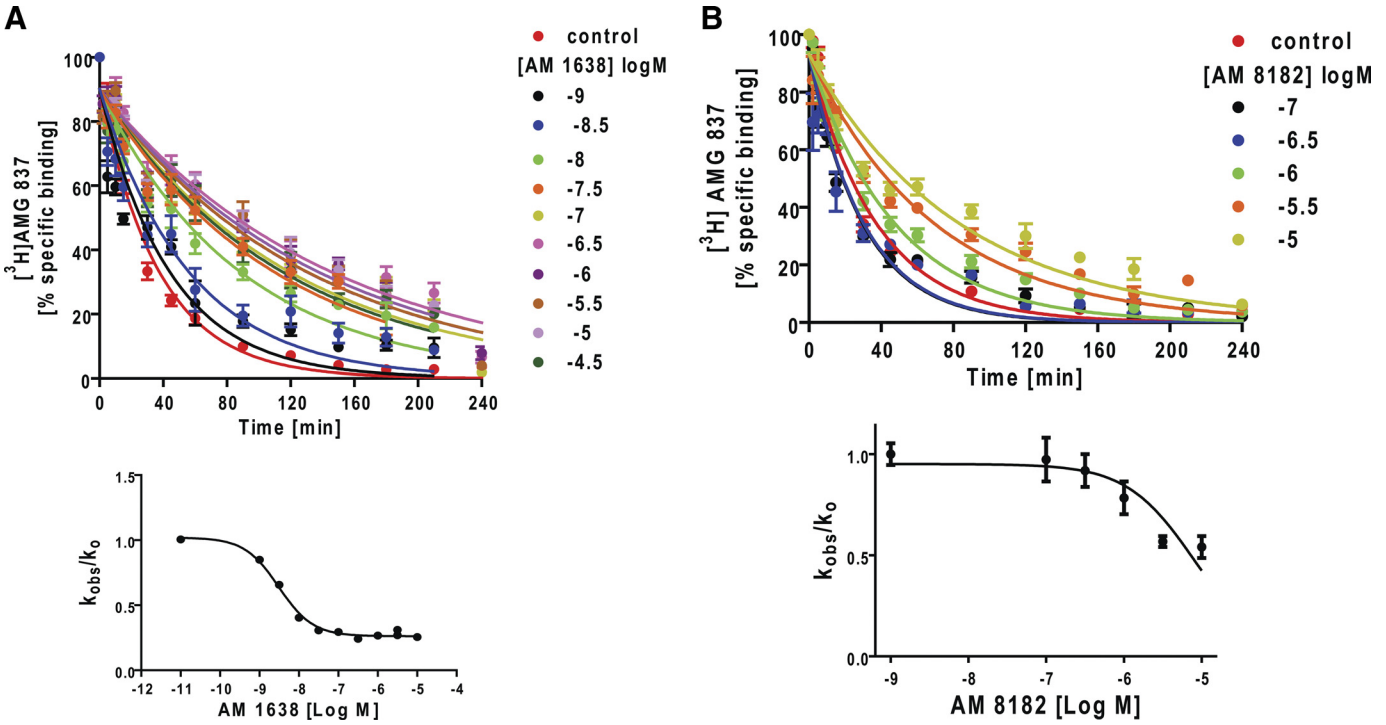

Fig. 7. Effects of AM 1638 and AM 8182 on [^{3}H]AMG 837 dissociation from the human FFA1 receptor. The dose-dependent effects on k_{off} of [^{3}H]AMG 837 in the presence of a series of concentrations of AM 1638 (A) or AM 8182 (B) are illustrated. The curves represent the best fits to a monoexponential decay. Data are presented as the percentage of the specific binding at the time of initiation of the measurement of dissociation. The control shown represents dissociation of [^{3}H]AMG 837 in the absence of any allosteric ligand. The data points represent means ± S.E.M. of three to six independent experiments, performed in duplicate. The insets depict the log dose-response curves for the effects of the allosteric ligands on radioligand dissociation. The observed dissociation constants (k_{obs}) have been normalized to the control dissociation rate constant (k_0) measured in the absence of a modulator. The estimated log affinities of AM 1638 and AM 8182 for the [^{3}H]AMG 837 occupied receptor are 8.51 ± 0.06 and 5.10 ± 0.05, respectively.

effect of the full agonist and the positive cooperative effects were abolished in the islets from FFA1 receptor knockout mice (J. Zhang, D.C.-H. Lin, unpublished data).

The positive functional cooperativity, seen in the AMG 837-AM 8182 interactions, is also observed when AMG 837-AM 1638 interactions were investigated. The presence of increasing fixed concentrations of the partial agonist AMG 837 increases the potency of the full agonist AM 1638 in the aequorin, IP accumulation, and ERK assays (Fig. 10, A–C, respectively) with estimated overall functional cooperativity values of 4- to 17-fold when the data were analyzed using the operational version of the allosteric ternary complex model. These cooperativity values are greater than the positive cooperativity seen in the binding assays ($\alpha = \sim 3$).

By measuring AMG 837 dose-response curves in the presence of different concentrations of AM 8182, we observe that the E_{max} of AMG 837 is enhanced with no decrease in potency of AMG 837 (Supplemental Figs. 4 and 5). These changes reflect the increase in efficacy of AMG 837 in the ternary complex. If AM 8182 were to bind at the same site as AMG 837, one would expect that the potency of AMG 837 would decrease in the presence of high concentrations of full agonist, which is not observed. Analysis of the data in Supplemental Figs. 4 and 5 by a recast form of the operational version of the allosteric ternary complex model gives cooperativities comparable to those shown in Table 4 for the analysis of the data in Fig. 8, A and B.

The large positive cooperative effects seen in the functional assays were also observed in the mouse islet insulin secretion assay, in which the potency of AM 1638 was enhanced approximately 40-fold in presence of 3 μM AMG 837 (Fig. 10D).

These results indicate that AMG 837 binds at a site on the receptor different from those for AM 1638 and AM 8182 and induces positive cooperative effects in the functional assays with these ligands even when, as in the case of AM 8182, the binding interaction is negatively cooperative.

Agonists AM 1638 and AMG 837 Act Allosterically with the Endogenous Ligand DHA in Functional Assays. The data from our equilibrium binding studies clearly show that DHA exhibits slight positive cooperativity with AM 1638 ($\alpha = \sim 2$) and is negatively cooperative with AMG 837 ($\alpha = \sim 0.1$) (Fig. 4; Table 3). We extended these findings to investigate their cooperative interactions with DHA in functional studies.

In the presence of increasing concentrations of DHA, the potency of AM 1638 was progressively left-shifted more than 7-fold in the aequorin assay (Fig. 11A) and more than 5-fold in the IP accumulation assay (Fig. 11B). These results, in conjunction with the binding interaction data, indicate that the efficacy of the two agonists in the DHA-receptor-AM 1638 complex is increased somewhat, relative to that of the binary complexes.

In the presence of different concentrations of AMG 837, the potency of DHA was also left-shifted in the aequorin and IP accumulation assays (Fig. 11, C and D, respectively). The values of the potencies and cooperativities when the data were analyzed by the operational version of the allosteric ternary complex model are listed in Table 4. As found for the other agonist combinations, the efficacy of the agonists in the ternary complex is increased relative to those in the binary complexes.

We also investigated the effect of different concentrations

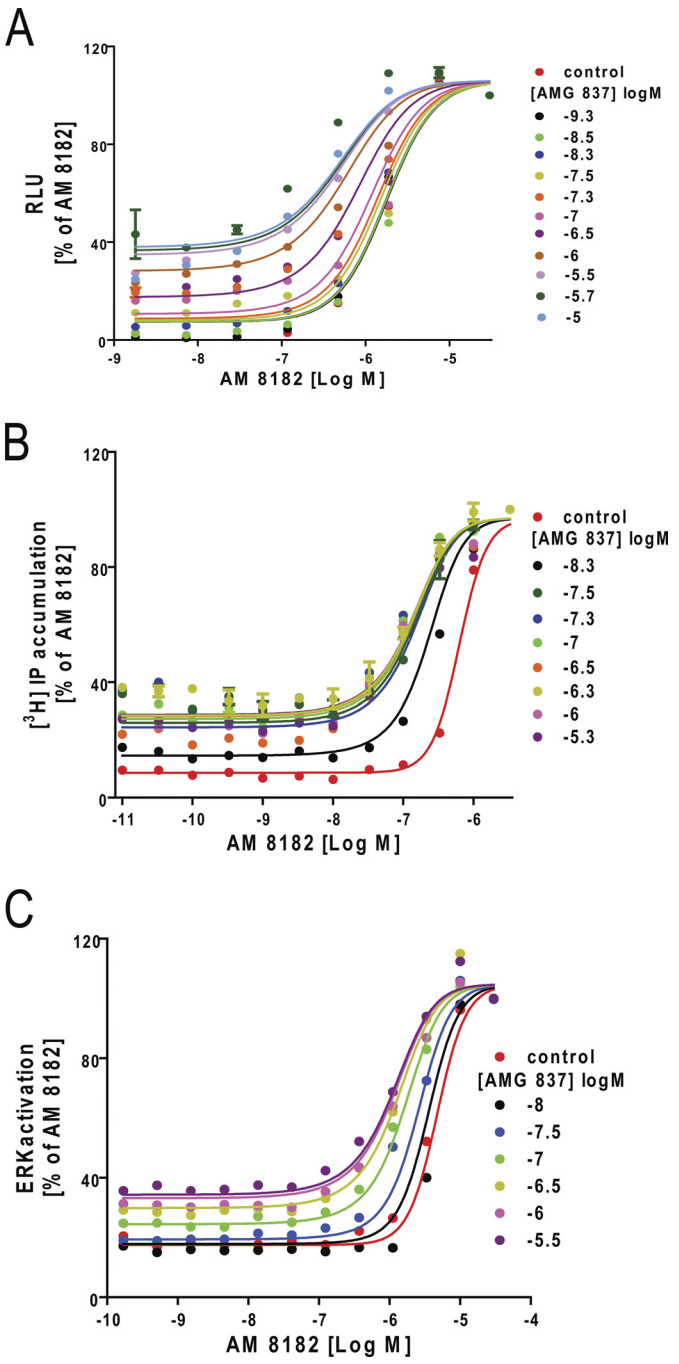

Fig. 8. The synthetic full agonist AM 8182 shows positive cooperativity with the partial agonist AMG 837 in functional assays. The effects of increasing concentrations of AMG 837 on the dose-response curve of AM 8182 are illustrated in the aequorin assay (A), the IP accumulation assay (B), and the ERK assay (C). The data have been normalized to the maximal response of AM 8182. All the data points are means ± S.E.M. of two to four independent experiments. The curves represent the best global fits using the operational model for the interaction of allosteric agonists. Positive cooperative effects of AMG 837 on AM 8182 activity are observed in all three assays, as evidenced by the leftward shifts of the dose-response curves. The mean parameters for $\log\tau_B$ (partial agonism of AMG 837) and $\log(\alpha\beta)$ (functional cooperativity) are reported in Table 4. RLU, relative luminescence units.

of DHA on the dose-response curve of AMG 837. Even high concentrations of DHA did not decrease the potency of AMG 837 and only increased the E_{max} (Supplemental Fig. 5). Analysis of these data by the recast form of the operational version of the allosteric ternary complex model gives cooperativities comparable to those shown in Table 4 for the analysis of the data in Fig. 11, C and D.

Evidence for Allosteric Effect between AMG 837 and LA in Mouse Islets. In vitro activation of FFA1 receptor by fatty acids has been shown to increase glucose-stimulated insulin secretion (Itoh et al., 2003). Hence, we looked at the effect of AMG 837 on glucose-stimulated insulin secretion in the absence and presence of a subthreshold concentration of LA (500 μM). LA alone produced no significant response but enhanced the potency of AMG 837 9-fold and increased in the efficacy of AMG 837 (Fig. 12). This increase in efficacy (E_{max}) is comparable with that observed in the in vitro functional assays using DHA as the endogenous ligand (Supplemental Fig. 5). These results confirm that the endogenous fatty acids bind at a different site than the partial agonist, AMG 837, exhibiting different cooperativities between binding and functional assays.

Evidence for Positive Allosteric Effects of Synthetic Full Agonists (AM 1638 and AM 8182) with the Partial Agonists AMG 837 and AM 6331 in In Vivo HF/STZ Rodent Models. Selective small molecule agonists of FFA1

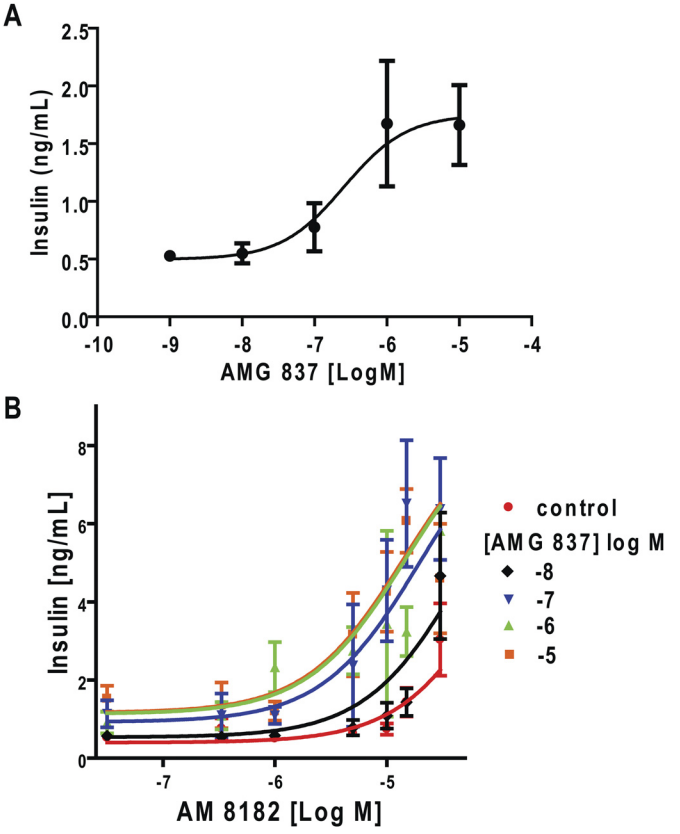

Fig. 9. Effects of AM 8182 and AMG 837 and their combination on insulin secretion in isolated mouse islets. A, dose-response curves for the stimulation of insulin release by AMG 837. The curve is a best-fit curve with a $\log EC_{50}$ of -6.6 ± 0.5 and a 2.5-fold stimulation of insulin release over basal release. Values shown are means ± S.E.M. of four independent experiments performed in duplicate. B, dose-response curves for insulin secretion in pancreatic islets stimulated by the full agonist AM 8182 in the presence and absence of fixed concentrations of AMG 837 are shown. The data are from four independent experiments performed in duplicate. The fit shown is that using the operational model for the interaction of allosteric agonists with $\log\tau_B$ (partial agonism of AMG 837) of -1.0 ± 0.2, $\log(\alpha\beta)$ (functional cooperativity) of 0.9 ± 0.2 and log affinity of AMG 837 of 7.3 ± 0.2. The log potency of AM 8182 was 4.0 ± 0.2.

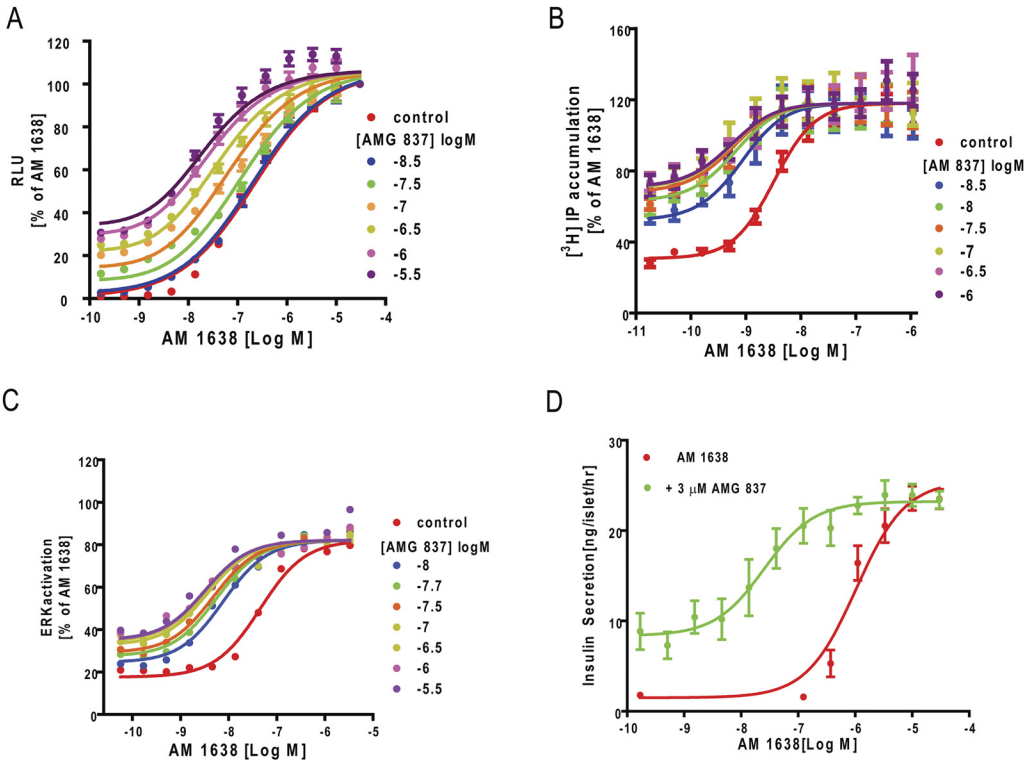

Fig. 10. The full agonist AM 1638 interacts with positive cooperativity with the partial agonist AMG 837 in functional assays. The effects of increasing concentrations of AMG 837 on the dose-response curve of AM 1638 are illustrated in the aequorin assay (A), the IP accumulation assay (B), the ERK assay (C), and the mouse islet insulin release assay (D). The data in A, B, and C have been normalized to the maximal response of AM 1638. All the data points are means ± S.E.M. of three independent experiments. The curves represent the best global fits using the operational model for the interaction of allosteric agonists. Positive cooperative effects of AMG 837 on AM 1638 activity are observed in all three assays, as evidenced by the leftward shifts of the dose-response curves. The mean parameters for $\log\tau_B$ (partial agonism of AMG 837) and $\log(\alpha\beta)$ (functional cooperativity) are reported in Table 4. D, effect of AM 1638 on insulin secretion in the absence or presence of 3 μM AMG 837. The data are from four independent experiments performed in duplicate. The curves represent best fits of the data using a simple dose-response equation (slope factor 1) with the log potency of AM 1638 being enhanced approximately 40-fold the presence AMG 837 (from −6.00 ± 0.12 to −7.59 ± 0.19) without the E_{max} being significantly changed. RLU, relative luminescence units.

TABLE 4
Cooperative interactions in functional assays

Interaction	Log (Functional Cooperativity) ± S.E.M. (*n*)		
	Aequorin	IP Accumulation	ERK
AMG 837/AM 8182			
Log($\alpha\beta$)	0.56 ± 0.07 (4)	0.47 ± 0.06 (4)	0.46 ± 0.05 (4)
log $\tau_{(AMG\ 837)}$	−0.21 ± 0.03	−0.24 ± 0.03	−0.28 ± 0.03
AMG 837/AM 1638			
Log($\alpha\beta$)	1.54 ± 0.06 (6)	0.96 ± 0.20 (6)	1.31 ± 0.08 (5)
log $\tau_{(AMG\ 837)}$	−0.48 ± 0.06	−0.06 ± 0.07	−0.46 ± 0.11
AMG 837/ DHA			
Log($\alpha\beta$)	0.53 ± 0.03 (4)	0.65 ± 0.04 (3)[a]	N.D.
log $\tau_{(AMG\ 837)}$	−0.43 ± 0.11	−0.10 ± 0.04	
DHA/AM 1638			
Log($\alpha\beta$)	>0.9 (3)	>0.7 (5)	N.D.
Log $\tau_{(AMG\ 837)}$			
AM 8182/AMG 837 (Supplemental Fig. 4)			
Log($\alpha\beta$)	0.97 ± 0.07 (2)	0.33 ± 0.05 (2)	N.D.
log $\tau_{(AMG\ 837)}$	−0.27 ± 0.04	−0.06 ± 0.01	
DHA/AMG 837 (Supplemental Fig. 5)			
Log($\alpha\beta$)	0.61 ± 0.07 (2)	−0.10 ± 0.05 (2)	N.D.
log $\tau_{(AMG\ 837)}$	−0.38 ± 0.04	−0.22 ± 0.01	

N.D., not determined.
[a] Slope factor constrained to 1.

receptor have been shown to promote glucose-dependent insulin secretion and reduce blood glucose in rodent models (Tan et al., 2008; Doshi et al., 2009). The effect of the combination of AM 6331 (a partial agonist with structure and properties similar to those of AMG 837) (see Supplemental Figs. 1 and 3) at 10 mg/kg and AM 8182 at 30 and 100 mg/kg was examined (Fig. 13, A and B). The agonists, on their own, had no effect on the insulin and blood glucose responses to a bolus administration of glucose except for the higher dose of AM 8182, which significantly reduced blood glucose levels

(but did not elevate insulin levels) at 15, 30, and 60 min ($P < 0.05$, unpaired two-tailed t test and $P < 0.001$, two-way ANOVA). The most striking observation was the enhancement of plasma insulin levels and the further reduction of glucose levels with AM 6331 in combination with the higher dose of AM 8182 ($P < 0.001$ and $P < 0.02$, respectively, for the two responses versus vehicle at all time points). The reduction in glucose levels with the higher dose combination versus those with AM 8182 alone was also significant at all time points ($P < 0.01$). The lower dose combination also generated a significant reduction in glucose levels at all time points ($P < 0.001$ versus vehicle) and in elevation of insulin levels at 0 and 60 min ($P < 0.001$). This can be interpreted as a positive allosteric functional interaction between AM 6331, a partial agonist structurally related to AMG 837 and known to act in a similar allosteric manner (Y. Xiong, G. Swaminath, Q. Cao, H. Salmonis, J. Lu, J. Houze, P.J. Dransfield, Y. Wang, J. Liu, S. Wong, et al., submitted for publication), and AM 8182.

We have shown that the partial agonist AMG 837 exhibits positive cooperativity with AM 1638 in binding, functional, and islet insulin secretion experiments. We explored the allosteric effects of this drug combination in HF/STZ mice during an oral glucose tolerance test (Fig. 14, A and B). In these experiments, AM 1638 alone, at the higher dose levels, significantly increased insulin levels and decreased blood glucose levels ($P < 0.01$ at all time points between 0 and 60 min) and produced significant functional effects at the lower dose level ($P < 0.01$ for lowering of blood glucose levels at all time points). This improvement in glycemia in this model was greater than that observed with AM 8182, probably because AM 1638 was approximately 50 times more potent than AM 8182 on the FFA1 receptor and acting through a different site.

Although AMG 837 acts as partial agonist on the FFA1 receptor in all the in vitro and ex vivo assays, we nevertheless observed that it had a significant effect in lowering plasma glucose through enhanced insulin secretion in these rodent models (Fig. 14, A and B). As shown in Fig. 14A, the combination of AMG 837 with the lower dose of AM 1638 induced a greater enhancement of insulin secretion at all times points compared with the responses of the synthetic agonists alone. The effects of this drug combination on blood glucose levels was even more pronounced, with significantly greater lowering being produced at all time points ($P < 0.05$), compared with those for the vehicle.

Selective Effects of Mutations of Two Arginine Residues on the Activation of FFAR1 by Synthetic Agonists. On the basis of mutational, modeling, and computational studies, two arginine residues, Arg183(5.39) and Arg258(7.35) in transmembrane regions 5 and 7, respectively, have been postulated to be key residues in both receptor activation and in the binding of the carboxyl group present in most FFAR1 agonists (Sum et al., 2007, 2009;

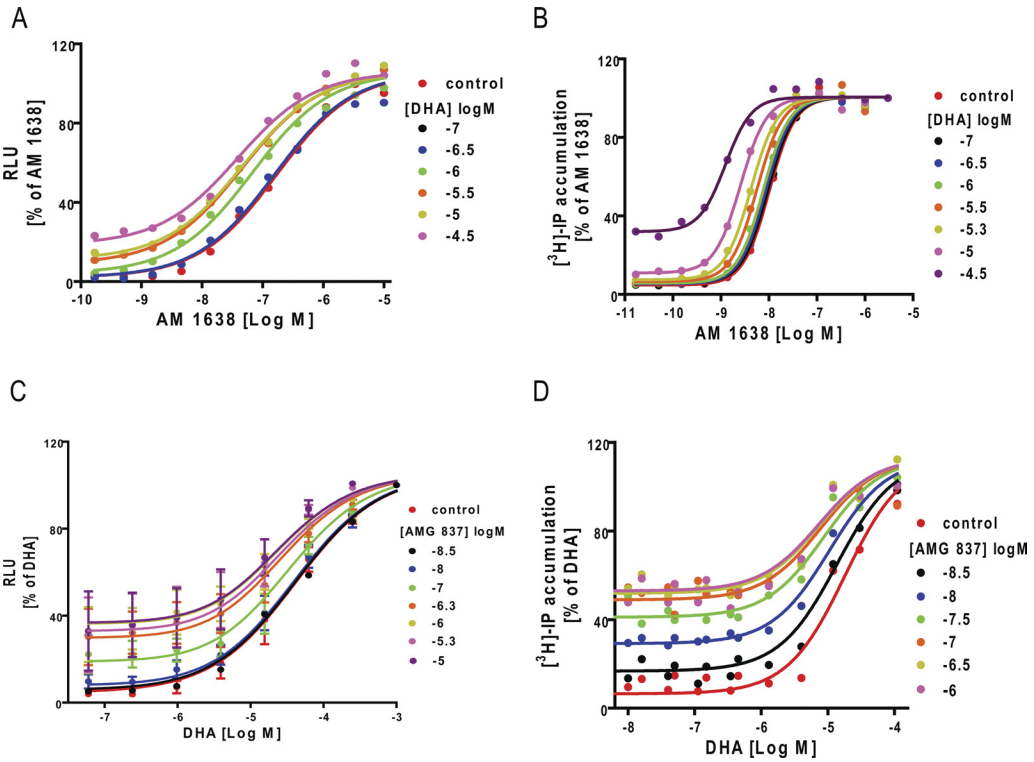

Fig. 11. Synergism of AM 1638 (A and B) and AMG 837 (C and D) with DHA in in vitro assays. Dose-response curves to AM 1638 were generated in the presence of increasing concentrations of DHA in aequorin (calcium release) assays (A) and IP accumulation assays (B). Data are normalized to the percentage of response of the highest concentration of AM 1638. The two sets of curves represent fits to a dose-response equation with the slope factors and the E_{max} values shared. At the highest concentration of AM 1638, the DHA dose-response curves are shifted 5- and 7-fold, respectively, in the aequorin and IP assays. These values provide a lower limit of $\alpha\beta$, which is listed in Table 4. Allosteric modulation of dose-response curves of DHA curves by fixed concentrations of AMG 837 in the aequorin (C) and IP accumulation (D) assays are shown. The data are normalized to the percentage of response of the highest concentration of DHA. All the data points shown are means ± S.E.M. of three to five independent experiments. Positive cooperative effects of AMG 837 on DHA activity are observed in both assays, as evidenced by the leftward shifts of the dose-response curves. The two sets of curves represent the best global fits using the operational model for the interaction of allosteric agonists. The mean parameters for $\log\tau_B$ (partial agonism of AMG 837) and $\log(\alpha\beta)$ (functional cooperativity) are reported in Table 4. RLU, relative luminescence units.

Tikhonova et al., 2007; Smith et al., 2009). Because the synthetic agonists reported here all contain a carboxyl group (Fig. 1), the effects of mutation of these residues to alanine and glutamine have been examined in an aequorin assay using transiently transfected CHO cells. The levels of expression of the receptors were estimated by FACS analysis (see *Materials and Methods* and Fig. 15).

The responses to the three synthetic agonists AMG 837, AM 1638, and AM 8182, which are proposed to bind to different sites on the receptor, were measured and compared with those of the endogenous agonist DHA (Fig. 15; Table1). For the wild-type receptor, the $-\log EC_{50}$ values were somewhat different from those reported in Table 1, with the agonists, in general, being more potent in the transient transfection assay. The exception was AMG 837, which was still a partial agonist, but the E_{max} had increased from 30 ± 3 to 58 ± 1% of the E_{max} of AM 1638. Some of these differences may be ascribed to differences in receptor expression levels in the two systems.

The R183A and R258A mutants could not be activated by AMG 837, but the R183Q and R258Q mutants were activated to a very small extent (6%) at the highest agonist concentration. In contrast, the AM 1638 responses were either unaffected or only slightly attenuated in the four mutants (up to 4-fold). The response to DHA was decreased to a small extent in all mutants (3–5-fold) with the AM 8182 response being decreased somewhat more (6–20-fold). For the Arg258 mutants, the alanine substitution produced a greater decrease in potency (approximately 3-fold) than the glutamine substi-

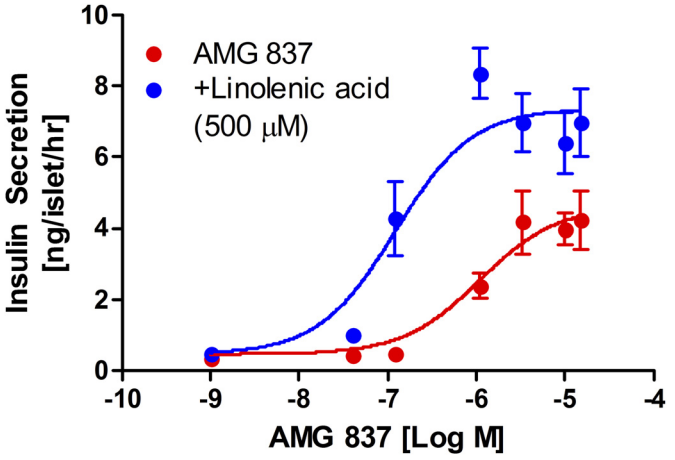

Fig. 12. Allosteric potentiation by the endogenous fatty acid, LA of the stimulation of insulin secretion in mouse pancreatic islets by the partial agonist AMG 837. AMG 837 alone activated insulin secretion, but 500 μM LA did not generate significant stimulation. The combination of AMG 837 and LA (500 μM) potentiated both the maximum response by approximately 60% and the potency of AMG 837 by approximately 9-fold. Data points represent the mean ± S.E.M. obtained from six independent experiments conducted in duplicate. The curves represent best fits of a simple dose-response relationship (slope factor 1) to the data.

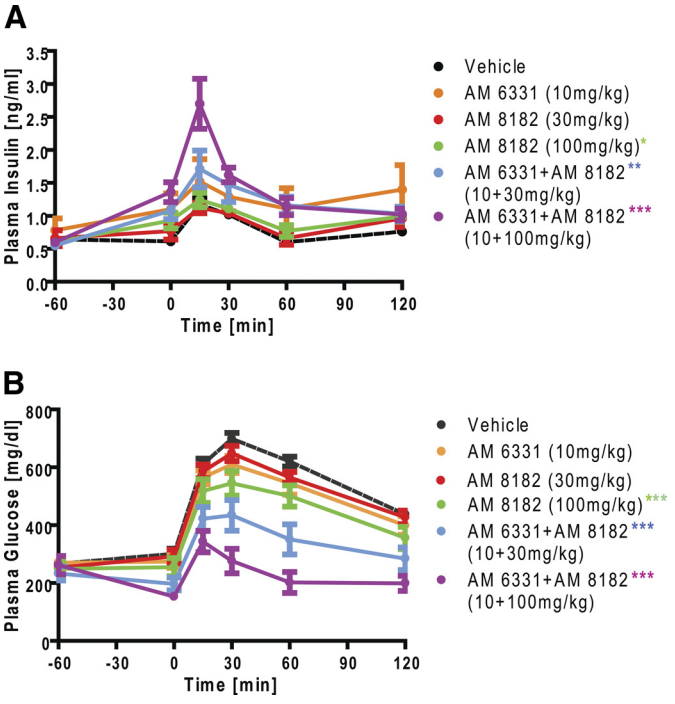

Fig. 13. Potentiation effects of acute administration of the synthetic agonists AM 6331 and AM 8182 in an oral glucose tolerance test in vivo. The test measured agonist potentiation of glucose-stimulated insulin secretion (A) and reduction of plasma glucose levels (B) in HF/STZ mice. AM 6331was administered at 10 mg/kg and AM 8182 at 30 and 100 mg/kg alone and in combination. Experimental details are described under *Materials and Methods*. All values are means ± S.E.M.; n = 8/group. There is a large enhancement of plasma insulin levels and reduction of glucose levels with AM 6331 in combination with the higher dose of AM 8182. The data were analyzed by two-way ANOVA followed by Student's t tests (**, $P < 0.01$; ***, $P < 0.0001$). More details, including the results of statistical analyses, are described in the main text.

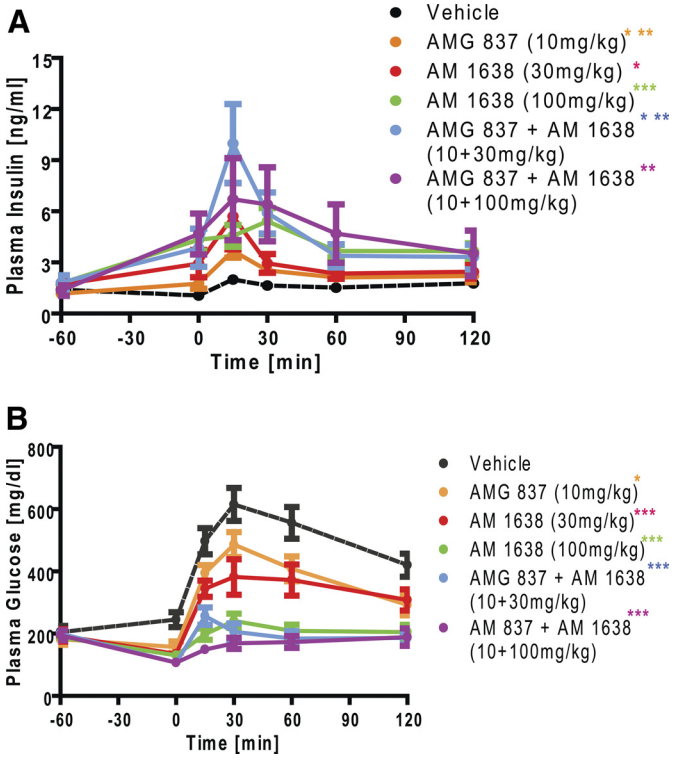

Fig. 14. Potentiation effects of acute administration of the synthetic agonists AMG 837 and AM 8182 in an oral glucose tolerance test in vivo. A, addition of different concentrations of AM 1638 to a fixed concentration of AMG 837 enhanced glucose-mediated insulin secretion. B, the positive allosteric effect of AM 1638 in presence of AMG 837 improves glucose tolerance in HF/STZ mice. Experimental details are described under *Materials and Methods*. Each point is the mean ± S.E.M.; n = 8/group. ***, $P < 0.0001$; **, $P < 0.01$; *, $P < 0.05$ versus vehicle and AM 1638 alone by Student's t test and by two-way ANOVA (***, $P < 0.0001$). There is a large enhancement of plasma insulin levels and reduction of glucose levels with AMG 837 in combination with the lower dose of AM 8182. More details, including the results of statistical analyses, are described in the text. RLU, relative luminescence units.

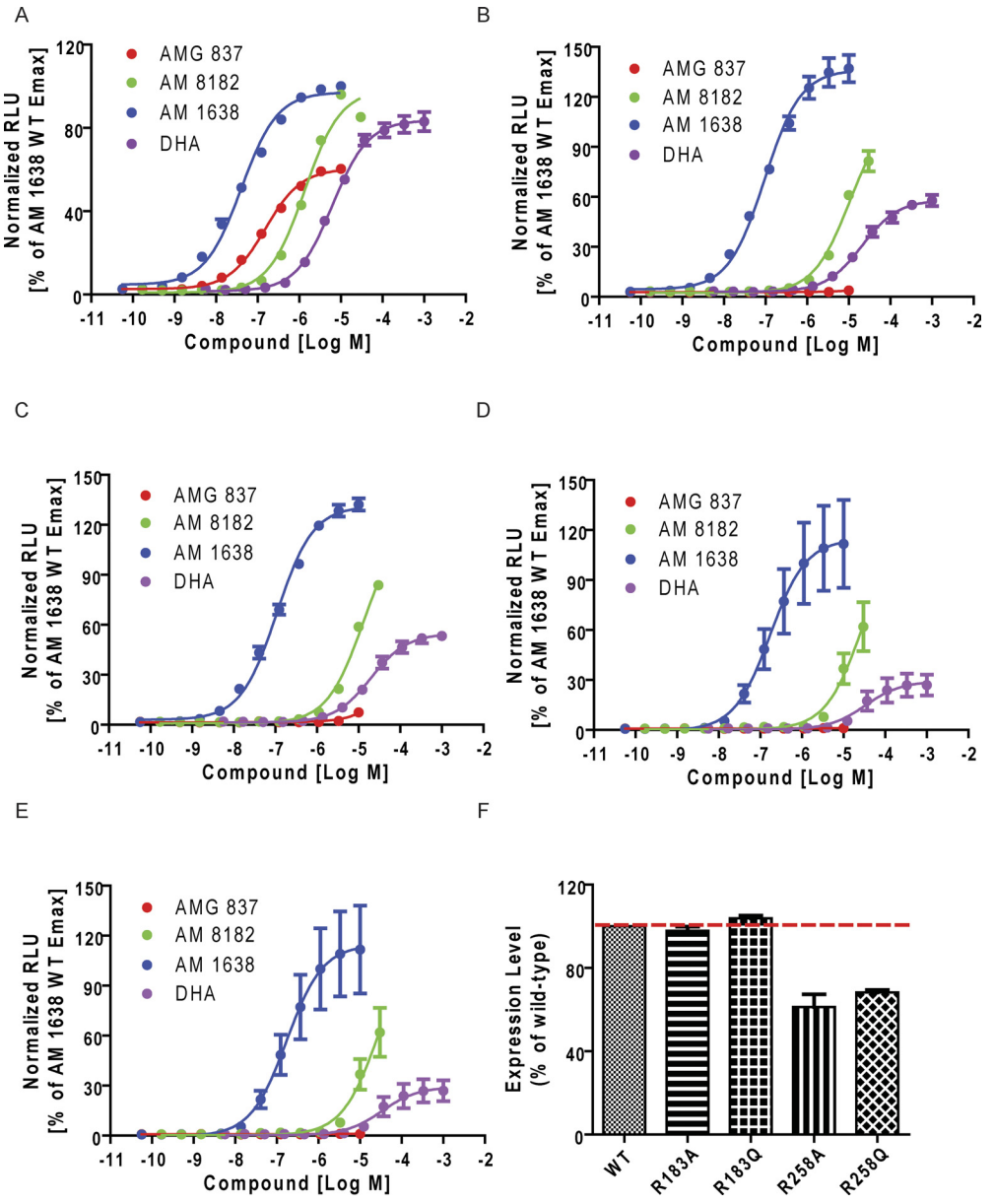

Fig. 15. Functional activity in an aequorin assay of FFA1 agonists on arginine mutants in transmembrane 5 (Arg183) and transmembrane 7 (Arg258) of FFA1. Wild-type (WT) and mutant constructs were transiently transfected into CHO cells. A, wild type receptor. B, R183A. C, R183Q. D, R258A. E, R258Q. Data are normalized to the maximum response of AM 1638 from the wild-type receptor and are shown as means ± S.E.M. of three to six independent experiments performed in duplicate. RLU, relative luminescence units.

tution. For Arg183, no difference between the A and Q mutants was observed.

Discussion

Several synthetic agonists for the FFA1 receptor have recently been identified (Christiansen et al., 2008; Bharate et al., 2009; Hara et al., 2009; Zhou et al., 2010; Lin et al., 2011; Sasaki et al., 2011; Tsujihata et al., 2011; Walsh et al., 2011). Antagonists have also been described (Briscoe et al., 2006; Humphries et al., 2009; Hu et al., 2010).

Until now, however, the complexity of the binding and functional properties of the FFA1 receptor has not been appreciated. Whereas allosteric sites on many GPCRs have been described (for reviews, see May et al., 2007; Bridges and Lindsley, 2008; Conn et al., 2009), including multiple allosteric sites such as those on muscarinic acetylcholine receptors (for a review, see Birdsall and Lazareno, 2005), there has been no previous description of allosteric interactions at the FFA1 receptor. Here, we have identified three novel synthetic ligands, two of which (AM 8182 and AM 1638) behave as full agonists and one (AMG 837) of which is a partial agonist in three different assay systems (Fig. 2).

Binding Cooperativity. The important feature of these agonists is that they interact allosterically with each other and at three different binding sites. The radiolabeled agonists, [^{3}H]AMG 837 and [^{3}H]AM 1638, label two different sites in a 1:1 stoichiometry (Fig. 5, A and C). AM 1638 enhances the affinity of [^{3}H]AMG 837 approximately 3-fold (Fig. 3), and the reciprocal enhancement of [^{3}H]AM 1638 by AMG 837 has been demonstrated (Fig. 4). The increase in affinity is not accompanied by any increase in the number of binding sites, B_{max} (Fig. 5, B and D). These binding data satisfy the predictions of the allosteric ternary complex model for the simple 1:1 allosteric interaction (Lazareno and Birdsall, 1995) and represent one of the few examples for which reciprocal two-way allosteric interactions in GPCRs have been characterized using radioligands for two interacting sites. Furthermore, AM 1638 slows down the dissociation

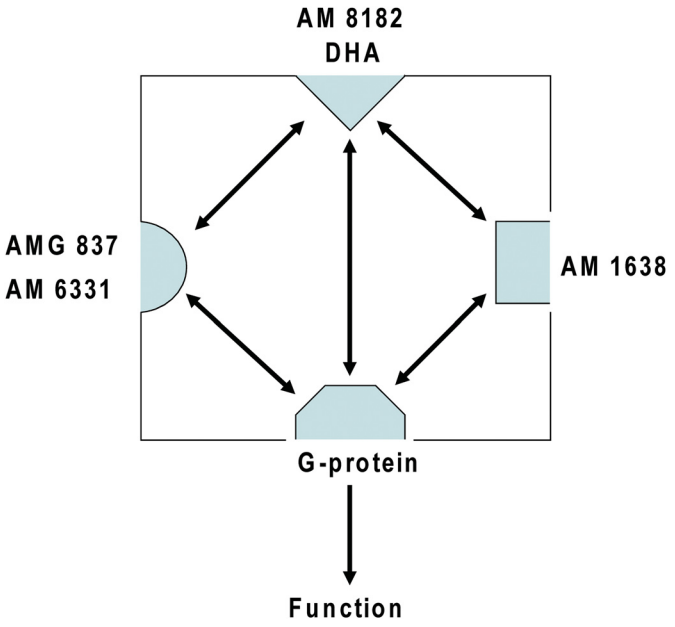

Fig. 16. Schematic model of the three binding sites on the FFA1 receptor and the ligands that interact at these sites and the G protein binding site. The allosteric interactions that facilitate the ability of ligands that bind to these sites to modulate receptor function are shown as double-headed arrows.

TABLE 5

Estimates of β, the increase in stimulus produced by the ligand combinations

Values were taken from Tables 3 and 4. Mean log $\tau_{(AMG\ 837)} = -0.27 \pm 0.04$ (12).

Interaction	Mean Log($\alpha\beta$) ± S.E.M. (n)	Mean Logα ± S.E.M. (n)	β Estimate
AMG 837/AM 8182	0.56 ± 0.11 (5)	−1.20 ± 0.24(2)	50
AMG 837/AM 1638	1.27 ± 0.17 (3)	0.45 ± 0.07 (5)	6
AMG 837/DHA	0.45 ± 0.15 (4)	−1.0	30
DHA/AM 1638	>0.7	0.3	>2.5

kinetics of [^{3}H]AMG 837 (Fig. 7A) with the potency predicted by the equilibrium data and the allosteric ternary complex model (Lazareno and Birdsall, 1995; Lazareno et al., 1998).

The third synthetic ligand, AM 8182, also interacts allosterically with [^{3}H]AMG 837, but with negative cooperativity (Fig. 4), and exhibits the predicted potency in slowing down the dissociation rate of [^{3}H]AMG 837 (Fig. 7B). This finding might suggest that AM 8182 was binding to the same site as AM 1638. However, AM 8182 has no effect on the binding of [^{3}H]AM 1638 (Fig. 4), which indicates neutral cooperativity between AM 8182 and AM 1638; i.e., AM 8182 is allosteric with *both* AM 1638 and AMG 837 and thus binds to a third binding site.

An important question is which of these sites might bind endogenous fatty acids, e.g., DHA? Binding studies show that DHA is allosteric with [^{3}H]AMG 837 (negatively cooperative) (Fig. 3) and exhibits slight positive cooperativity with [^{3}H]AM 1638 (Fig. 4). Thus, DHA, like AM 8182, does not bind to either of the two sites labeled by the radioligands. It was possible to exploit the lack of effect of AM 8182 on [^{3}H]AM 1638 binding and its known affinity to inhibit [^{3}H]AMG 837 binding to demonstrate that increasing concentrations of AM 8182 shift the DHA enhancement curves of [^{3}H]AM 1638 binding in a parallel fashion and to the extent expected of a competitive interaction between AMG182 and DHA (Fig. 6). This result confirms the presence of three interacting sites, shown illustratively in Fig. 16.

Functional Cooperativity. The allosteric interactions were also manifest in functional studies. A surprising, and potentially therapeutically useful, finding is that the agonists for the three different sites enhance each others' actions in simple in vitro assays (Figs. 8, 10, and 11), even when the binding interactions exhibit negative cooperativity in binding (e.g., AMG 837-DHA and AMG 837-AM 8182 interactions). The functional interaction data fit very well to the operational model of allosteric agonism (Leach et al., 2007).

The important parameter describing the functional allosteric interaction in this model is the composite parameter, $\alpha\beta$, which reflects the magnitude of the functional cooperativity factor for the interaction of two ligands in a given assay and is a measure of the overall change in agonist potency and efficacy due to the agonists forming the ternary complex. A value of $\alpha\beta > 1$ (positive functional cooperativity) is manifest as an increase in potency of the full agonist (Figs. 8, 10, and 11) and an increase in E_{max} of the partial agonist (Supplemental Figs. 4 and 5). Of interest, the values of $\alpha\beta$ for a given interaction between two ligands are very similar in the three in vitro assays used (aequorin, IP accumulation, and ERK assays) (Table 4), and there is no evidence of ligand-directed signaling for these ligands in these assays.

Because α is the cooperativity factor seen in binding studies, if the interactions obey the predictions of the allosteric ternary complex model, the value of β (the change in stimulus to the system provided by A and B in the presence of the other ligand) can thus be calculated. Estimates of β derived from mean values of logα and log($\alpha\beta$) are given in Table 5 and show the very large increases in stimulus (approximately 30–50-fold) provided by the biliganded receptor for AMG 837-AM 8182 and AMG 837-DHA combinations and smaller increases (approximately 3–6-fold) for AM 1638-DHA and AM 1638-AMG 837 combinations.

For the AMG 837-AM 8182 and AMG 837-LA combinations, the positive functional cooperativity has also been detected in a more relevant assay of the stimulation of insulin release in pancreatic islets (Figs. 9 and 12, respectively). Finally the combinations of AM 6331-AM 8182 and AMG 837-AM 1638 potentiate insulin release and lowering of blood glucose levels in vivo (Figs. 13 and 14).

The observed positive functional cooperativity is not surprising, given that each of the agonist-receptor complexes formed will have an increased proportion of active state, relative to the ground state. In a sense, each monoliganded receptor behaves as a constitutively active receptor, with the binding of a second agonist molecule to a different allosteric site producing an enhanced response in terms of its potency and efficacy. It has therefore been possible for the first time, to our knowledge, to demonstrate the activation of a GPCR from any one of three different binding sites.

Structure-Activity Relationships. One really surprising feature of these three groups of synthetic agonists shown in Fig. 1 is that they appear superficially to be so similar in structure and yet so different in their binding selectivities for the three sites. A detailed description of the SAR will be reported elsewhere. At the simplest level, however, the structures shown in Fig. 1 differ in 1) the presence of a *meta*-biphenyl ring system (AMG 837) versus a *para*-biphenyl ring system (AM 8182, AM 6331, and AM 1638), 2) *para*-substi-

TABLE 6
Functional potencies of the FFA1 agonists on wild-type receptor compared with FFAR1 mutants

Constructs	−Log EC_{50} ± S.E.M. (*n*)			
	AMG 837	AM 1638	AM 8182	DHA
Wild-type	6.81 ± 0.03	7.39 ± 0.02	5.87 ± 0.02	5.20 ± 0.04
R183A	Inactive	7.02 ± 0.04 (0.37)[a]	4.98 ± 0.05 (0.89)[a]	4.68 ± 0.05 (0.52)[a]
R183Q	6 ± 1% stimulation at 10^{-5} M	6.93 ± 0.03 (0.46)[a]	4.89 ± 0.03 (0.98)[a]	4.70 ± 0.05 (0.5)[a]
R258A	Inactive	6.76 ± 0.18 (0.63)[a]	4.56 ± 0.24 (1.31)[a]	4.47 ± 0.20 (0.73)[a]
R258Q	6 ± 1% stimulation at 10^{-5} M	7.28 ± 0.17 (0.11)[a]	5.11 ± 0.13 (0.76)[a]	4.76 ± 0.13 (0.44)[a]

[a] Differences in log EC_{50} between the wild-type and arginine mutants.

tution of the isolated phenyl ring (AMG 837, AM 6331, and AM 8182) versus *meta*-substitution (AM 1638), and 3) the presence of the 3-phenyl-hex-4-ynoic acid head group (AMG 837 and AM 6331) versus the 3-phenyl-hex-4-eneoic head group (AM 8182) or the 3-phenyl-2-cyclopropyl-propionic acid head group (AM 1638), both with stereochemistry opposite to that of the head group of the partial agonists.

One can speculate that the presence of the 3-phenyl-hex-4-ynoic acid head group contributes to the partial agonism of AMG 837 and AM 6331 and their selectivity for their allosteric site. A *para*-biphenyl versus *meta*-biphenyl tail appears not to be crucial for this activity. AM 8182, although it possesses a *para*-biphenyl ring, has a different head group than AM 6331 or AMG 837, which results in it behaving like an agonist and binding to the same site as DHA. AM 1638 possesses a third type of head group in combination with a different orientation of the substitution on the isolated phenyl ring. One or both of these features may contribute to its selectivity for its allosteric site.

FFA1 has an extraordinarily flat SAR for short-, medium-, and long-chain fatty acids of very different structures, with functional potencies varying by no more than approximately 20-fold for more than 40 endogenous fatty acids (Briscoe et al., 2003). Could this receptor have evolved multiple binding sites to sense different fatty acids? Could these three sites, which have been found in this study, bind different fatty acids? If so, then corelease of more than one fatty acid will give a highly amplified signal if the fatty acids bind to different sites. This would be a natural mechanism for endogenous signal amplification and increased sensitivity, and a rationale for the evolution of the multiple binding sites.

Location of the Allosteric Sites. Most FFA1 ligands are carboxylic acids, and it has been suggested that a cluster of hydrophilic residues in transmembrane regions 5, 6, and 7 [Arg183(5.39), Asn244(6.55), and Arg258(7.35)] interact with the carboxyl group of these ligands and with that of linoleic acid (Sum et al., 2007). This hypothesis is based on modeling studies and the abolition of, or very much reduced, potency of the synthetic agonist 4-[[(3-phenoxyphenyl)methyl]amino-]benzenepropanoic acid (GW9508) for the alanine mutants. These residues are less important for linoleic acid, for which agonist potency for the alanine mutants is only reduced 2- to 5-fold, and this raises the question of whether GW9508 and linoleic acid bind to the same site. It has also been suggested that the two arginine residues form ionic locks with Glu145 and Glu172 in the extracellular loops of FFA1 (Sum et al., 2009; Hudson et al., 2011). Upon agonist binding to one or both arginines, it is proposed that the locks are broken and that this leads to receptor activation.

In agreement with this hypothesis, mutation of the two arginine residues profoundly attenuated the functional activity of AMG 837 (Fig. 15; Table 6). However, the functional activities of AM 8182, AM 1638, and DHA were only slightly affected, This result indicates minor, and possibly indirect, effects of the mutations of the arginines on the binding and activity of the latter ligands and is in accord with the alternative modes of binding, demonstrated in the binding and functional studies reported here.

Because uncharged amide and substituted amide derivatives of FFA1 carboxylic acid ligands do not have dramatically reduced potencies (Garrido et al., 2006) and certain diacyl phloroglucinols are also FFA1 agonists (Bharate et al., 2008), it is possible that one or more of these binding modes does not necessarily involve a direct interaction of the ligand with an arginine residue.

The overall picture is clearly more complicated than previously recognized. The results of a mutagenesis and modeling study to attempt to determine the modes of binding of the different classes of FFA1 agonists to the three binding sites on the FFA1 receptor will be reported elsewhere.

Therapeutic Potential. The large positive functional cooperativity between the synthetic ligands (up to 30-fold) allows lower doses of a combination of ligands to be used to achieve a given level of stimulation than would be required for a single ligand alone. Up to a 30-fold lower dose of one ligand or up to 10-fold lower doses of both ligands can generate a given response and should reduce potential unwanted effects. This is illustrated in Fig. 10C in which threshold doses of 1.5 nM AM 1638 and 20 nM AMG 837, when applied in combination, produce an response equivalent to approximately 30 nM AMG 1638 and >300 nM AMG 837 when administered singly.

The FFA1 receptor agonists reported here may not only be pharmacological tools but also have the potential utility for the treatment of type 2 diabetes and have implications in pathophysiological settings of the receptor.

Acknowledgments

We are very grateful to Professor Arthur Christopoulos (Monash University, Victoria, Australia) for providing eq. 2 used to analyze the functional interaction data. We are also thankful to Jenny Lu, Jeff Reagan, and Ralf Schwandner for providing the stable cell lines.

Authorship Contributions

Participated in research design: Birdsall and Swaminath.
Conducted experiments: Lin, Guo, Luo, Zhang, Nguyen, Chen, Tran, and Swaminath.
Contributed new reagents or analytic tools: Dransfield, Brown, Vimolratana, Jiao, Wang, and Houze.
Performed data analysis: Birdsall and Swaminath.
Wrote or contributed to the writing of the manuscript: Birdsall and Swaminath.

References

Allderdice PW, Miller OJ, Miller DA, Warburton D, Pearson PL, Klein G, and Harris H (1973) Chromosome analysis of two related heteroploid mouse cell lines by quinacrine fluorescence. *J Cell Sci* **12:**263–274.

Alquier T, Peyot ML, Latour MG, Kebede M, Sorensen CM, Gesta S, Ronald Kahn C, Smith RD, Jetton TL, Metz TO, et al. (2009) Deletion of GPR40 impairs glucose-induced insulin secretion in vivo in mice without affecting intracellular fuel metabolism in islets. *Diabetes* **58:**2607–2615.

An S, Bleu T, Zheng Y, and Goetzl EJ (1998) Recombinant human G protein-coupled lysophosphatidic acid receptors mediate intracellular calcium mobilization. *Mol Pharmacol* **54:**881–888.

Araki T, Hirayama M, Hiroi S, and Kaku K (2012) GPR40-induced insulin secretion by the novel agonist TAK-875: first clinical findings in patients with type 2 diabetes. *Diabetes Obes Metab* **14:**271–278.

Bharate SB, Nemmani KV, and Vishwakarma RA (2009) Progress in the discovery and development of small-molecule modulators of G-protein-coupled receptor 40 (GPR40/FFA1/FFAR1): an emerging target for type 2 diabetes. *Expert Opin Ther Pat* **19:**237–264.

Bharate SB, Rodge A, Joshi RK, Kaur J, Srinivasan S, Kumar SS, Kulkarni-Almeida A, Balachandran S, Balakrishnan A, and Vishwakarma RA (2008) Discovery of diacylphloroglucinols as a new class of GPR40 (FFAR1) agonists. *Bioorg Med Chem Lett* **18:**6357–6361.

Birdsall NJ and Lazareno S (2005) Allosterism at muscarinic receptors: ligands and mechanisms. *Mini Rev Med Chem* **5:**523–543.

Black JW and Leff P (1983) Operational models of pharmacological agonism.*Proc R Soc Lond B Biol Sci* **220:**141–162.

Bridges TM and Lindsley CW (2008) G-protein-coupled receptors: from classical modes of modulation to allosteric mechanisms. *ACS Chem Biol* **3:**530–541.

Briscoe CP, Peat AJ, McKeown SC, Corbett DF, Goetz AS, Littleton TR, McCoy DC, Kenakin TP, Andrews JL, Ammala C, et al. (2006) Pharmacological regulation of insulin secretion in MIN6 cells through the fatty acid receptor GPR40: identification of agonist and antagonist small molecules. *Br J Pharmacol* **148:**619–628.

Briscoe CP, Tadayyon M, Andrews JL, Benson WG, Chambers JK, Eilert MM, Ellis C, Elshourbagy NA, Goetz AS, Minnick DT, et al. (2003) The orphan G protein-coupled receptor GPR40 is activated by medium and long chain fatty acids. *J Biol Chem* **278:**11303–11311.

Brown SP, Cao Q, Dransfield PJ, Du X, Fu Z, Houze J, Jiao XY, Kim YJ, Kohn TJ, Lai S, et al. (2011), inventors; Amgen Inc., assignee. Substituted biphenyl GPR40 modulators. U.S. Patent 8,030,354. 2011 Oct 4.

Christiansen E, Urban C, Grundmann M, Due-Hansen ME, Hagesaether E, Schmidt J, Pardo L, Ullrich S, Kostenis E, Kassack M, et al. (2011) Identification of a potent and selective free fatty acid receptor 1 (FFA1/GPR40) agonist with favorable physicochemical and in vitro ADME properties. *J Med Chem* **54:**6691–6703.

Conn PJ, Christopoulos A, and Lindsley CW (2009) Allosteric modulators of GPCRs: a novel approach for the treatment of CNS disorders. *Nat Rev Drug Discov* **8:**41–54.

Costanzi S, Neumann S, and Gershengorn MC (2008) Seven transmembrane-spanning receptors for free fatty acids as therapeutic targets for diabetes mellitus: pharmacological, phylogenetic, and drug discovery aspects. *J Biol Chem* **283:** 16269–16273.

Doshi LS, Brahma MK, Sayyed SG, Dixit AV, Chandak PG, Pamidiboina V, Motiwala HF, Sharma SD, and Nemmani KV (2009) Acute administration of GPR40 receptor agonist potentiates glucose-stimulated insulin secretion in vivo in the rat. *Metab Clin Exp* **58:**333–343.

Garrido DM, Corbett DF, Dwornik KA, Goetz AS, Littleton TR, McKeown SC, Mills WY, Smalley TL Jr, Briscoe CP, and Peat AJ (2006) Synthesis and activity of small molecule GPR40 agonists. *Bioorg Med Chem Lett* **16:**1840–1845.

Hara T, Hirasawa A, Sun Q, Sadakane K, Itsubo C, Iga T, Adachi T, Koshimizu TA, Hashimoto T, Asakawa Y, et al. (2009) Novel selective ligands for free fatty acid receptors GPR120 and GPR40. *Naunyn Schmiedebergs Arch Pharmacol* **380:**247–255.

Herrington J, Zhou YP, Bugianesi RM, Dulski PM, Feng Y, Warren VA, Smith MM, Kohler MG, Garsky VM, Sanchez M, et al. (2006) Blockers of the delayed-rectifier potassium current in pancreatic beta-cells enhance glucose-dependent insulin secretion. *Diabetes* **55:**1034–1042.

Hu H, He LY, Gong Z, Li N, Lu YN, Zhai QW, Liu H, Jiang HL, Zhu WL, and Wang HY (2010) A novel class of antagonists for the FFAs receptor GPR40. *Biochem Biophys Res Commun* **390:**557–563.

Hudson BD, Smith NJ, and Milligan G (2011) Experimental challenges to targeting poorly characterized GPCRs: uncovering the therapeutic potential for free fatty acid receptors. *Adv. Pharmacol* **62:**175–218.

Humphries PS, Benbow JW, Bonin PD, Boyer D, Doran SD, Frisbie RK, Piotrowski DW, Balan G, Bechle BM, Conn EL, et al. (2009) Synthesis and SAR of 1,2,3,4-tetrahydroisoquinolin-1-ones as novel G-protein-coupled receptor 40 (GPR40) antagonists. *Bioorg Med Chem Lett* **19:**2400–2403.

Itoh Y and Hinuma S (2005) GPR40, a free fatty acid receptor on pancreatic β cells, regulates insulin secretion. *Hepatol Res* **33:**171–173.

Itoh Y, Kawamata Y, Harada M, Kobayashi M, Fujii R, Fukusumi S, Ogi K, Hosoya M, Tanaka Y, Uejima H, et al. (2003) Free fatty acids regulate insulin secretion from pancreatic β cells through GPR40. *Nature* **422:**173–176.

Kebede M, Alquier T, Latour MG, Semache M, Tremblay C, and Poitout V (2008) The fatty acid receptor GPR40 plays a role in insulin secretion in vivo after high-fat feeding. *Diabetes* **57:**2432–2437.

Lan H, Hoos LM, Liu L, Tetzloff G, Hu W, Abbondanzo SJ, Vassileva G, Gustafson EL, Hedrick JA, and Davis HR (2008) Lack of FFAR1/GPR40 does not protect mice from high-fat diet-induced metabolic disease. *Diabetes* **57:**2999–3006.

Latour MG, Alquier T, Oseid E, Tremblay C, Jetton TL, Luo J, Lin DC, and Poitout V (2007) GPR40 is necessary but not sufficient for fatty acid stimulation of insulin secretion in vivo. *Diabetes* **56:**1087–1094.

Lazareno S and Birdsall NJ (1995) Detection, quantitation, and verification of allosteric interactions of agents with labeled and unlabeled ligands at G protein-coupled receptors: interactions of strychnine and acetylcholine at muscarinic receptors. *Mol Pharmacol* **48:**362–378.

Lazareno S, Gharagozloo P, Kuonen D, Popham A, and Birdsall NJ (1998) Subtype-selective positive cooperative interactions between brucine analogues and acetylcholine at muscarinic receptors: radioligand binding studies. *Mol Pharmacol* **53:** 573–589.

Leach K, Sexton PM, and Christopoulos A (2007) Allosteric GPCR modulators: taking advantage of permissive receptor pharmacology. *Trends Pharmacol Sci* **28:**382–389.

Lin DC, Zhang J, Zhuang R, Li F, Nguyen K, Chen M, Tran T, Lopez E, Lu JY, Li XN, et al. (2011) AMG 837: a novel GPR40/FFA1 agonist that enhances insulin secretion and lowers glucose levels in rodents. *PLoS One* **6:**e27270.

May LT, Leach K, Sexton PM, and Christopoulos A (2007) Allosteric modulation of G protein-coupled receptors. *Annu Rev Pharmacol Toxicol* **47:**1–51.

Nagasumi K, Esaki R, Iwachidow K, Yasuhara Y, Ogi K, Tanaka H, Nakata M, Yano T, Shimakawa K, Taketomi S, et al. (2009) Overexpression of GPR40 in pancreatic β-cells augments glucose-stimulated insulin secretion and improves glucose tolerance in normal and diabetic mice. *Diabetes* **58:**1067–1076.

Naik H, Vakilynejad M, Wu J, Viswanathan P, Dote N, Higuchi T, and Leifke E (2012) Safety, tolerability, pharmacokinetics, and pharmacodynamic properties of the GPR40 agonist TAK-875: results from a double-blind, placebo-controlled single oral dose rising study in healthy volunteers. *J Clin Pharmacol* **52:**1007–1016.

Sasaki S, Kitamura S, Negoro N, Suzuki M, Tsujihata Y, Suzuki N, Santou T, Kanzaki N, Harada M, Tanaka Y, et al. (2011) Design, synthesis, and biological activity of potent and orally available G protein-coupled receptor 40 agonists. *J Med Chem* **54:**1365–1378.

Sawzdargo M, George SR, Nguyen T, Xu S, Kolakowski LF, and O'Dowd BF (1997) A cluster of four novel human G protein-coupled receptor genes occurring in close proximity to CD22 gene on chromosome 19q13.1. *Biochem Biophys Res Commun* **239:**543–547.

Smith NJ, Stoddart LA, Devine NM, Jenkins L, and Milligan G (2009) The action and mode of binding of thiazolidinedione ligands at free fatty acid receptor 1. *J Biol Chem* **284:**17527–17539.

Steneberg P, Rubins N, Bartoov-Shifman R, Walker MD, and Edlund H (2005) The FFA receptor GPR40 links hyperinsulinemia, hepatic steatosis, and impaired glucose homeostasis in mouse. *Cell Metab* **1:**245–258.

Stoddart LA, Brown AJ, and Milligan G (2007) Uncovering the pharmacology of the G protein-coupled receptor GPR40: high apparent constitutive activity in guanosine 5′-*O*-(3-[^{35}S]thio)triphosphate binding studies reflects binding of an endogenous agonist. *Mol Pharmacol* **71:**994–1005.

Stoddart LA, Smith NJ, and Milligan G (2008) International Union of Pharmacology. LXXI. Free fatty acid receptors FFA1, -2, and -3: pharmacology and pathophysiological functions. *Pharmacol Rev* **60:**405–417.

Sum CS, Tikhonova IG, Costanzi S, and Gershengorn MC (2009) Two arginine-glutamate ionic locks near the extracellular surface of FFAR1 gate receptor activation. *J Biol Chem* **284**: 3529–3536.

Sum CS, Tikhonova IG, Neumann S, Engel S, Raaka BM, Costanzi S, and Gershengorn MC (2007) Identification of residues important for agonist recognition and activation in GPR40. *J Biol Chem* **282:**29248–29255.

Swaminath G (2008) Fatty acid binding receptors and their physiological role in type 2 diabetes. *Arch Pharm (Weinheim)* **341:**753–761.

Swaminath G, Steenhuis J, Kobilka B, and Lee TW (2002) Allosteric modulation of β_2-adrenergic receptor by Zn^{2+}. *Mol Pharmacol* **61:**65–72.

Tahara A, Matsuyama-Yokono A, and Shibasaki M (2011) Effects of antidiabetic drugs in high-fat diet and streptozotocin-nicotinamide-induced type 2 diabetic mice. *Eur J Pharmacol* **655:**108–116.

Tan CP, Feng Y, Zhou YP, Eiermann GJ, Petrov A, Zhou C, Lin S, Salituro G, Meinke P, Mosley R, et al. (2008) Selective small-molecule agonists of G protein-coupled receptor 40 promote glucose-dependent insulin secretion and reduce blood glucose in mice. *Diabetes* **57:**2211–2219.

Tikhonova IG, Sum CS, Neumann S, Thomas CJ, Raaka BM, Costanzi S, and Gershengorn MC (2007) Bidirectional, iterative approach to the structural delineation of the functional "chemoprint" in GPR40 for agonist recognition. *J Med Chem* **50:**2981–2989.

Tsujihata Y, Ito R, Suzuki M, Harada A, Negoro N, Yasuma T, Momose Y, and Takeuchi K (2011) TAK-875, an orally available G protein-coupled receptor 40/free fatty acid receptor 1 agonist, enhances glucose-dependent insulin secretion and improves both postprandial and fasting hyperglycemia in type 2 diabetic rats. *J Pharmacol Exp Ther* **339:**228–237.

Walker SD, Borths CJ, DiVirgilio E, Huang L, Liu P, Morrison H, Sugi K, Tanaka M, Woo JCS, and Faul MM (2011) Development of a scalable synthesis of a GPR40 agonist. *Org Process Res Dev* **15:**570–580.

Walsh SP, Severino A, Zhou C, He J, Liang GB, Tan CP, Cao J, Eiermann GJ, Xu L, Salituro G, et al. (2011) 3-Substituted 3-(4-aryloxyaryl)-propanoic acids as GPR40 agonists. *Bioorg Med Chem Lett* **21:**3390–3394.

Zhou C, Tang C, Chang E, Ge M, Lin S, Cline E, Tan CP, Feng Y, Zhou YP, Eiermann GJ, et al. (2010) Discovery of 5-aryloxy-2,4-thiazolidinediones as potent GPR40 agonists. *Bioorg Med Chem Lett* **20:**1298–1301.

Address correspondence to: Dr. Gayathri Swaminath, Amgen Inc., 1120 Veterans Blvd., South San Francisco, CA 94080. E-mail: gswamina@amgen.com